The author(s) shown below used Federal funds provided by the U.S. Department of Justice and prepared the following final report:

Document Title:	**Analysis of the Effect of a Variety of PCR Inhibitors on the Amplification of DNA using Real Time PCR, Melt Curves and STR Analysis**
Author(s):	**Bruce McCord, Arianna Pionzio, Robyn Thompson**
Document No.:	**249148**
Date Received:	**September 2015**
Award Number:	**2010-DN-BX-K204**

This report has not been published by the U.S. Department of Justice. To provide better customer service, NCJRS has made this federally funded grant report available electronically.

Opinions or points of view expressed are those of the author(s) and do not necessarily reflect the official position or policies of the U.S. Department of Justice.

Analysis of the effect of a variety of PCR inhibitors on the amplification of DNA using real time PCR, melt curves and STR analysis.

Award Number 2010-DN-BX-K204

Author(s) Bruce McCord, Arianna Pionzio, Robyn Thompson

Abstract

The goal of this project was to examine the effect of a variety of PCR inhibitors using real time PCR, melt curve analysis and STR typing in an attempt to define the inhibitory mechanism of these materials and to assist forensic analysts in interpreting their results. Furthermore, by examining the effect of these inhibitors on internal control sequences used in real time PCR, we hope to assist designers of real time PCR quantification kits in developing better probes for inhibition. We have examined the effects of simple treatments such as dilution, increasing polymerase, BSA and magnesium concentration on the inhibitory effects. Lastly we have measured the effects of different extractions on the success of removing inhibition. In general, our results clarify the role of PCR inhibitors in PCR amplification and their effects on STR amplification. We see three basic types of inhibitors – DNA binding, polymerase binding and mixed mode (inhibitors which affect both polymerase and template). We note that real time PCR amplification efficiency and melt curves help to elucidate the modes of inhibition and have some predictive power in defining downstream allele dropout. Furthermore we note that while allele sequence has an effect on sensitivity to PCR inhibition, the length of the amplicon is most important. Overall we find that PCR inhibition is a complex process that cannot be modeled by one specific compound. Individuals interested in validating new forensic methods should carefully choose a range of inhibitors to encompass the range of modes of inhibition.

Note: Portions of this document have been submitted to Journal of Forensic Sciences and FSI Genetics for publication.

This document is a research report submitted to the U.S. Department of Justice. This report has not been published by the Department. Opinions or points of view expressed are those of the author(s) and do not necessarily reflect the official position or policies of the U.S. Department of Justice.

Table of Contents

1. Abstract 1
2. Executive summary 3
3. Full Report 16

   Part I: An investigation of PCR inhibition using Plexor® based quantitative PCR and short tandem repeat amplification
4. Part II : The Effect of Internal Control Sequence and Length on the Response to PCR Inhibition in Real-Time PCR Quantitation 49
5. Part III: Conclusions 64
6. Part IV: Dissemination of Results 65

This document is a research report submitted to the U.S. Department of Justice. This report has not been published by the Department. Opinions or points of view expressed are those of the author(s) and do not necessarily reflect the official position or policies of the U.S. Department of Justice.

Executive Summary

Overview

A common problem in forensic genetic analysis is the presence of PCR inhibitors. Inhibitors are chemical and biological matrix interferences that coextract with DNA and affect downstream processing. These interfering substances present a challenge for forensic human identification due to inhibitory effects on short tandem repeat (STR) amplification that include poor peak balance, locus-specific drop-out, enhanced stutter, and poor sensitivity. The overall result can be no amplified product or partial profiles that are difficult to interpret. PCR inhibitors may be introduced at any stage prior to amplification of the sample. Potential sources for inhibition include humic and tannic acids in soil; calcium and collagen in bone and tissue; hematin in blood; bile salts and catabolic substances in feces and urine; and melanin in hair. In addition, chemical components such as urea, phenol, and transition metal ions may enter during the extraction process through inadvertent contamination. Whatever the source, inhibitors prevent or reduce the efficiency of PCR amplifications.

The goal of this project was to utilize real-time PCR amplification to monitor changes in efficiencies and melt curves of known PCR inhibitors and compare this data with STR amplification. Our hypothesis was that there is not one single mechanism for inhibition and that inhibitor type, DNA sequence, amplicon length and buffer composition all play a role in the response to PCR inhibition during STR amplification. What we saw was that measuring PCR efficiency, in combination with melt curve analysis, can be a very useful technique to understand inhibition. We discovered 3 specific mechanisms for inhibition: polymerase binding, which results in a general loss of amplification efficiency, DNA template binding which results in an increase in Ct and melt curve effects, and mixed mode binding, in which the PCR efficiency and melt temperatures are affected. Examining amplification efficiency across sequence and amplicon size, we found that as amplicon size increased, and amplicon GC content decreased, inhibitory effects become more detectable. However the effects of length were far more

This document is a research report submitted to the U.S. Department of Justice. This report has not been published by the Department. Opinions or points of view expressed are those of the author(s) and do not necessarily reflect the official position or policies of the U.S. Department of Justice.

important than sequence. These conclusions were also confirmed upon performing STR analysis. When a DNA sample is inhibited, STR analysis shows a gradual loss of larger amplicons as the concentration of inhibitor increases. In addition, depending on the type of inhibitor binding, different sequence specific allele losses occur with DNA binding and mixed mode inhibitors producing more complex patterns of inhibition than those inhibitors that primarily bind the polymerase.

These results affect forensic science and the triers of fact in important ways. With the increasing sensitivity of STR kits and the increasing application of these kits to mixed and degraded samples, it is critical to understand that PCR inhibition can produce effects such as allele dropout and imbalanced peaks. These effects complicate interpretation in unexpected ways due to the importance of length and sequence in the inhibition process. Great care must be taken in interpreting an inhibited sample, particularly if a mixture is present. Secondly, our results show clearly the important effect of inhibitor concentration on the PCR reaction. While not always a linear relationship, inhibition increases with concentration. Therefore dilution of the sample will often result in an improved amplification in spite of the reduction in peak intensity. We found other methods to reduce inhibition, such as the addition of extra BSA, magnesium and polymerase to the reaction, does not always reduce inhibition. In fact, the response of the reaction to these steps depends on the type of the inhibitor.

We can also make some recommendations to the manufacturers of real time PCR kits used in the detection of inhibition. The use of a long, low GC content DNA amplicon as an internal PCR control generally will provide an increased ability to detect inhibition during the real time PCR quantification step. Furthermore, our results suggest that it should be possible to tailor the composition of internal positive control sequences in quantification kits to a desired level of sensitivity by altering the length and sequence of the internal control sequences.

Introduction

Real-time PCR – or quantitative PCR (qPCR) – is an important analytical method for determining the quantity of recovered DNA in forensic samples because of its sensitivity, specificity, and ease of automation. Typically in real-time PCR amplification, a fluorescent dye is introduced during thermal

This document is a research report submitted to the U.S. Department of Justice. This report has not been published by the Department. Opinions or points of view expressed are those of the author(s) and do not necessarily reflect the official position or policies of the U.S. Department of Justice.

cycling, causing a change in fluorescent output as the double stranded DNA (dsDNA) product accumulates. The number of cycles required during amplification to reach a significant change in fluorescence is known as the cycle threshold (C_T). It is determined by a linear relationship between the log of the concentration of DNA template and the number of PCR cycles.

There are different approaches that can be used for fluorescence-based detection assays, including TaqMan® and Scorpion probes, SYBR Green intercalation, and the Plexor® HY System (Promega Corporation, Madison WI). While the result of TaqMan and SYBR Green analysis is an increase in fluorescence intensity that is proportional to the amount of amplicon produced, the Plexor® HY system produces a loss in signal as the product accumulates due to its quenching mechanism. Unlike other qPCR assays, which use probes or intercalating dyes, Plexor® HY does not interfere with or bind to the incipient DNA duplex, since its chemistry involves quenching between two labeled nucleotides, isoguanine (iso-dG) and 5'-methylisocytosine (iso-dC) at the distal end of the amplicon. The reaction includes the use of a fluorescently labeled iso-dC on the 5' end of one of the two primers. During the amplification process, the iso-dG that contains the quencher is specifically incorporated at a position complementary to the iso-dC in the opposite strand. Once this occurs, a reduction in the fluorescent signal occurs that is proportional to the quantity of dsDNA.

Since quenched amplicons produce a significant change in fluorescent signal as they are denatured, a melt curve can be produced at the end of the amplification cycle that is characteristic of the PCR product. The melting temperature (T_m) can be used to confirm that the amplified product is from the intended target DNA and contains the appropriate product length, sequence, and strand complementarity. In addition, nonspecific amplification products such as primer-dimer artifacts, mis-priming, and DNA inhibition will result in alterations to the melting temperature and curve.

PCR inhibitors that bind DNA should result in reproducible shifts in the melt curve. In addition, this type of PCR inhibition can be easily identified based on a shift in C_T when compared to uninhibited samples. To test for this, an internal (non-human) positive control sequence (IPC) is added to the real-time reaction mixture and the relative differences between the amplification of this control sequence in an

This document is a research report submitted to the U.S. Department of Justice. This report has not been published by the Department. Opinions or points of view expressed are those of the author(s) and do not necessarily reflect the official position or policies of the U.S. Department of Justice.

unknown sample and a DNA standard are assessed. The presence of a PCR inhibitor in the reaction mixture will produce a higher C_T value.

An alternative mechanism for PCR inhibition is to alter the efficiency (theoretical doubling) of *Taq* polymerase. *Taq* polymerase inhibition can be recognized by a change in the slope of the exponential curve produced by the real-time amplification. There is also a minor effect on the C_T value but this is the result of the change in slope and not a reduction in template availability. *Taq* polymerase inhibition has been modeled using parameters based on a Richards function as has been discussed by Guescini et al. [1]

A third type of PCR inhibition is caused by an inhibitor that both blocks the polymerase and effects the DNA template. We call this class of inhibitor a mixed mode inhibitor. It is characterized by a marked reduction in PCR efficiency curves and clear evidence of DNA binding through examination of the melt curve. Again losses in Taq polymerase efficiency can be detected by modeling or visual examination of the melt curve, where a decrease in slope is seen.

The most common effect of any inhibitor is unsuccessful genotyping, which results in either no STR profiles or partial profiles that are difficult to interpret. Inhibitors that affect *Taq* polymerase efficiency generally result in a generic loss of the larger loci. This may be the result of a slower base incorporation rate in the presence of inhibition. Inhibitors that bind DNA similarly result in loss of larger alleles but can also show locus-specific effects, resulting in a pattern of allele loss in which some loci are affected and others are not. This is presumably due to a preference of the inhibitor to bind specific sections of the template and not others. Mixed mode inhibitors show complex patterns of allele dropout similar to those seen with DNA binding inhibitors.

Experimentally, there are several approaches ranging from dilution to magnetic bead extraction that can result in some success in overcoming the effects of inhibition. However, many of these cleanup methods involve wash steps that may affect recovery of the template DNA, making them undesirable for samples containing low levels of DNA. Newer PCR multiplex kits have also been shown to be effective in reducing inhibition due to improved buffer formulations. However, these kits are still affected by inhibitors at higher concentrations. Thus it is important to understand and identify the mechanisms of

This document is a research report submitted to the U.S. Department of Justice. This report has not been published by the Department. Opinions or points of view expressed are those of the author(s) and do not necessarily reflect the official position or policies of the U.S. Department of Justice.

inhibition, in order to better interpret results obtained from such samples. This proposal compares the effects of a variety of PCR inhibitors using the Plexor® HY qPCR assay while monitoring amplification efficiency and slope, $C_{T,}$ and melt curves effect. A variety of inhibitors known to affect forensic samples were examined. These included calcium, humic acid, collagen, phenol, tannic acid, hematin, bile salts, melanin, EDTA, urea and guanidinium thiocyanate. Different DNA sequences were also compared to study the effects of amplicon length and sequence when amplification occurs in the presence of PCR inhibition.

Experimental Results

To perform these experiments standard real time PCR assays using the Plexor amplification kit (Promega) were performed with increasing amounts of inhibitors added to the reaction mixture. The range and concentration of these inhibitors is provided in Table 1. From previous results using Sybr Green based real time PCR detection we anticipated that different inhibitors would affect efficiency in a predictable fashion.

This document is a research report submitted to the U.S. Department of Justice. This report has not been published by the Department. Opinions or points of view expressed are those of the author(s) and do not necessarily reflect the official position or policies of the U.S. Department of Justice.

Inhibitor	**Concentration**	**C_T shift Range (cycles)**	**T_m shift range (°C)**	**Plexor® mode of inhibition**
Calcium	0, 0.5, 1.0 1.5, 2.0, 2.5 mM	25 - 37	80.4	*Taq* polymerase inhibitor
Tannic Acid	0, 5, 10, 15, 17.5, 20. 22.5 ng/µL	25 - 37	80.5 - 80.4	*Taq* polymerase inhibitor
Bile Salts	0, 0.25, 0.50, 0.75, 1.00, 1.25, 1.50 µg/µL	25 - 36	80.5 - 80.0	DNA binding inhibitor
Humic Acid	0, 5, 10, 15, 20, 25, 30 ng/µL	25 - 36	80.5 - 80.2	DNA binding inhibitor
Hematin	0, 15, 30, 45, 60, 75, 90, 105 µM	25 - 36	80.5 - 79.4	DNA binding inhibitor
Melanin	0, 10, 20, 30, 40, 50, 60 µg/µL	25 - 34	80.5 - 79.4	DNA binding inhibitor
EDTA	0, 0.4, 0.8, 1.2, 1.6, 2.0, 2.4 mM	25 - 34	80.5 - 78.2	DNA binding inhibitor
Phenol	0, 33, 66, 83, 100, 116, 133 µg/µL	25 - 30	80.5 - 79.1	Mixed mode inhibitor
Collagen	0, 25, 38, 50, 63, 75, 88, 100 ng/µL	25 - 30	80.7 - 84.3	Mixed mode inhibitor
Urea	0, 200, 400, 600, 800, 1000, 1200 mM	25 - 29	80.5 - 79.4	Mixed mode inhibitor
Guanidinium	0, 1.5, 3.0, 4.5, 6.0, 7.5, 9.0 µg/µL	25 - 28	80.6 - 83.5	Mixed mode inhibitor

Table 1: A list of different inhibitors tested, their effects on Ct, melt temperature and mode of action.

Modeling PCR inhibition

There are three different processes that produce PCR inhibition *:Taq* inhibition, which affects the exponential amplification curve; DNA binding, which produces changes in Ct with no effect on amplification efficiency; and mixed mode inhibition, which affects both efficiency and availability of template. We used curve fitting software with the Weibull model ($y = a - b*\exp(-cx^d)$), a four parameter model to predict the effects of different type PCR inhibition on the amplification efficiency curve (relative fluorescence vs Ct) [2]. The a and b values correspond to the initial and final fluorescence values, respectively, while the c value follows the changes in C_t. The d value in the model describes the

This document is a research report submitted to the U.S. Department of Justice. This report has not been published by the Department. Opinions or points of view expressed are those of the author(s) and do not necessarily reflect the official position or policies of the U.S. Department of Justice.

efficiency of the reactions, as it relates to the slope of the curve in the linear phase. Figure 1 illustrates how the two main modes of inhibition and their effect on real-time PCR kinetics can be modeled. Figure 1A illustrates the effect of inhibition on *Taq* polymerase using a model based on the effect of increasing concentrations of tannic acid. To produce this curve, the experimental results for tannic acid inhibition were modeled using the software. A decrease in the slope of the amplification curve is seen which can be modeled by gradually decreasing the exponential d term in the equation. Figure 1B illustrates the effect of loss of template due to inhibitor binding to DNA, as would be seen when increasing concentrations of bile salts are added to the reaction. Curve fitting performed on the bile salt results demonstrates that the slope and shape of the sigmoidal curve remains relatively constant but there is an increase in C_T. This effect can be produced by adjusting the c term in the equation. In both situations, as the concentration of inhibitor increases, a gradual loss of product produced at the conclusion of the PCR occurs (measured by changes in $F_{max,}$ the maximal fluorescence parameter). The results of this model illustrate how the measurement of PCR efficiency and Ct can be used to define the type of PCR inhibition in a more measurable way. This can be compared to the standard process in most forensic laboratories in which only Ct is monitored.

A 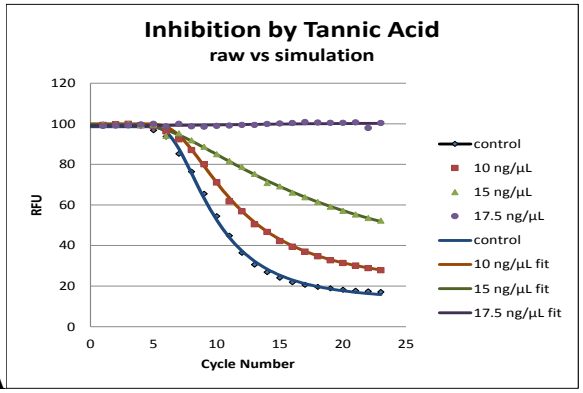

B 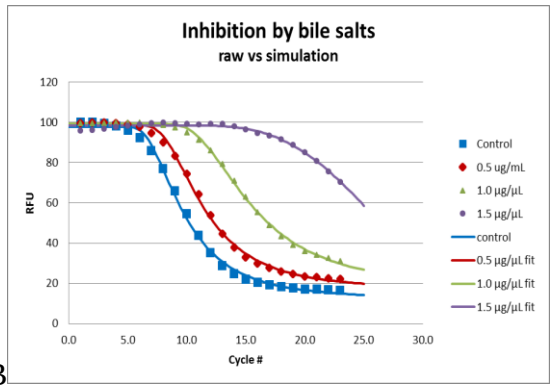

This document is a research report submitted to the U.S. Department of Justice. This report has not been published by the Department. Opinions or points of view expressed are those of the author(s) and do not necessarily reflect the official position or policies of the U.S. Department of Justice.

Figure 1. Comparison of two models of PCR inhibition curves using the Weibull Model at the following concentrations of bile salts: 0 µg (red), 0.5 µg/µl (blue), 1 µg/µl (green), 1.5 µg/µl (purple). 1A: Raw data and Weibull simulation of the effects of increasing concentrations of Tannic acid, a *Taq* polymerase inhibitor. 1B. Raw data and Weibull simulation of the effect of increasing concentration of bile salts, an inhibitor that binds to DNA, The fits were produced using CurveExpert software based on the raw data created by adding increasing concentrations of each inhibitor to the Plexor® HY real-time PCR Quantification kit. Values for each curve are listed in Table 2.

Examination of data for three different types of inhibitors in Table 2 shows that for tannic acid, the d term which is related to the exponential slope decreases with increasing inhibitor concentration. while it is quite stable in the bile salt example where the slope varies little until the concentration of the inhibitor reaches 1.5µg/ µL/µL.. Interestingly the c term decreases for tannic acid while in the bile salt sample the c term increases and the d term remains stable until inhibition reaches the highest levels. Phenol, a mixed mode inhibitor, produces a response much like tannic acid, as would be expected as this data reflects only the slope effects and does not reflect melt curve differences.

Table 2: A list of Weibull fit parameters determined for a set of Plexor® HY real-time autosomal amplification curves. The data show the effect of increased concentration of three PCR inhibitors (tannic acid, bile salts, and phenol) on the reaction curves.

Tannic acid	**a**	**b**	**c**	**d**
Control 0 ng/µL	99	86	1408	-3.35
10 ng/µL	99	82	1617	-3.37
15 ng/µL	99	83	807	-3.00
17.5 ng/µL	99	80	494	-2.68
20 ng/µL	100	82	249	-2.28
22.5 ng/µL	100	87	35.5	-1.30
Bile Salts	**a**	**b**	**c**	**d**
Control 0 µg/ µL	98	86	2333	-3.57
0.5 µg/µL	99	82	7641	-3.82
1 µg/µL	99	81	20208	-3.74
1.5 µg/µL	99	48	435	-1.60
Phenol	**a**	**b**	**c**	**d**
Control 0 µg/µL	99	87	2896	-3.61
33 µg/µL	98	86	1760	-3.33
66 µg/µL	99	84	2807	-3.50
83 µg/µL	99	82	993	-2.87
100 µg/µL	99	80	699	-2.60

This document is a research report submitted to the U.S. Department of Justice. This report has not been published by the Department. Opinions or points of view expressed are those of the author(s) and do not necessarily reflect the official position or policies of the U.S. Department of Justice.

Effects of Amplicon length and sequence

Another area of interest to us was the internal control sequence present in realtime PCR kits. Previous work had demonstrated the strong correlation of amplicon length with PCR inhibition. We had also seen effects from differences in amplicon sequence [3]. Thus a series of experiments were performed by replacing the standard internal control in the Plexor HY system with a randomly generated internal control sequence that varied in length and sequence. The goal of these experiments was to examine the overall ability of different internal control sequences to predict the presence of PCR inhibition. More specifically, we were interested in the ways variations in concentration of different PCR inhibitors impacted amplicons of different length and sequence. Our overall results indicated that the amplicon size can have more of an influence on the degree of inhibition than the specific amplicon sequence. The sequence can also have an effect if the inhibitor interacts more directly with the DNA, rather than with the polymerase. For example, Figure 2 demonstrates the effect of different concentrations of collagen on the real time PCR melt curve. The figure demonstrates that the relative degree of inhibition (reduction of slope of amplification and change in Ct) are affected by both sequence and amplicon length.

Amplicon size strongly impacts the degree of inhibition for all modes of inhibition in the real-time PCR amplification curves. The changes in efficiency between the 80bp amplicon and the 230bp for any sequence composition can show major differences when analyzing STRs. Typically, the largest amplicon fails at many inhibitory concentrations where the smallest amplicon amplifies rather well. This is presumably because the larger sequences require a longer interaction with the polymerase and provide a wider range of DNA sequence variations to bind to. This is an expected finding, as inhibitory events commonly cause larger STR loci to drop out first. Previous studies on STR dropout due to inhibition have indicated that the size of the STR can have a greater influence on allele drop out and peak imbalance than the %GC content of the STR [4]. However, as seen in these results, the pattern of inhibitory progression is not identical for all DNA or *Taq* inhibitors as sequence increases in length or GC content.

This document is a research report submitted to the U.S. Department of Justice. This report has not been published by the Department. Opinions or points of view expressed are those of the author(s) and do not necessarily reflect the official position or policies of the U.S. Department of Justice.

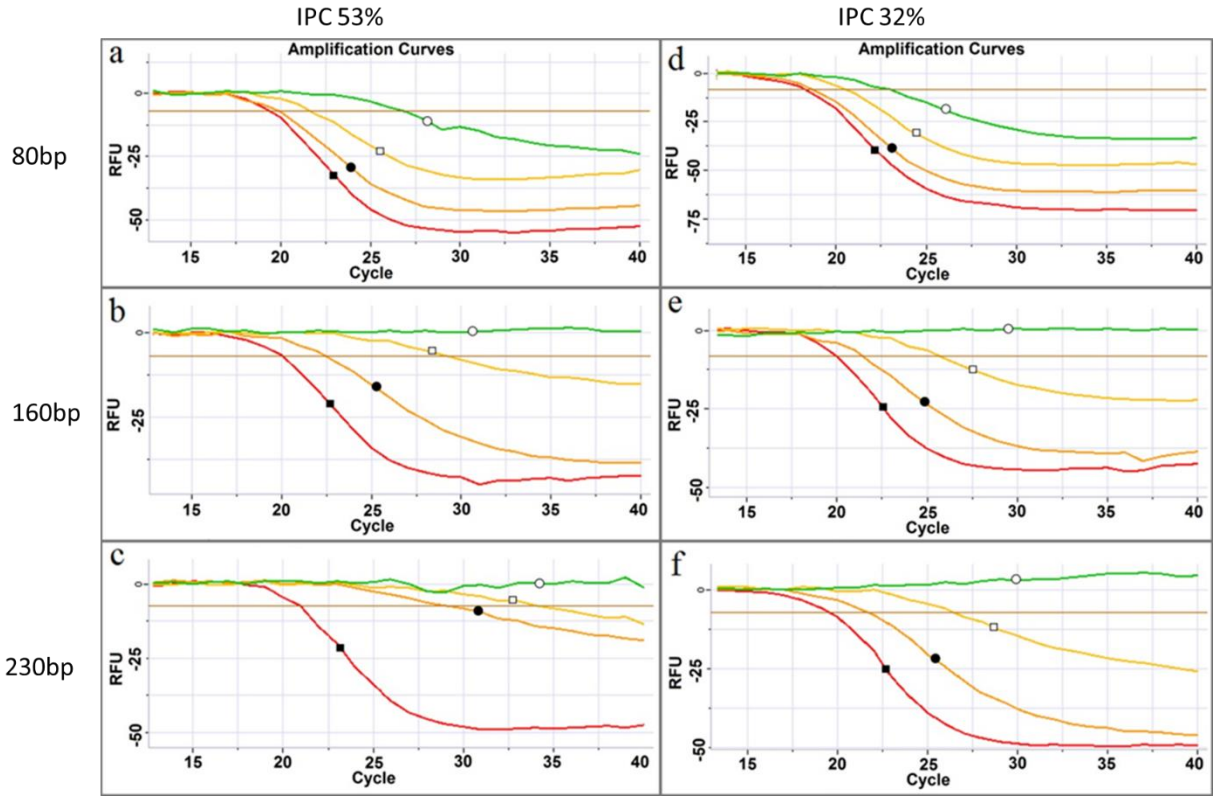

Figure 2: Effect of internal control amplicon size and sequence with the Plexor HY real time PCR quantification kit. The results demonstrate the effect of size and sequence on response to increasing concentrations of the collagen inhibitor. The amplification curves include sequences with 53% GC content (a-c) and 32% GC content (d-f). Amplicon size increases from top to bottom with panels (a, d) = 80bp; (b, e) = 160bp and (c, f) = 230bp. Quantity of inhibitor added ranges from 0 (red ■), 87.5 (orange ●), 100 (yellow □) and 112.5ng/µL (green ○). An optimal response would involve even spacing of the amplification curves between the different levels of inhibition. As can be seen from these curves the response to inhibition increases with amplicon size and varies with GC content.

This document is a research report submitted to the U.S. Department of Justice. This report has not been published by the Department. Opinions or points of view expressed are those of the author(s) and do not necessarily reflect the official position or policies of the U.S. Department of Justice.

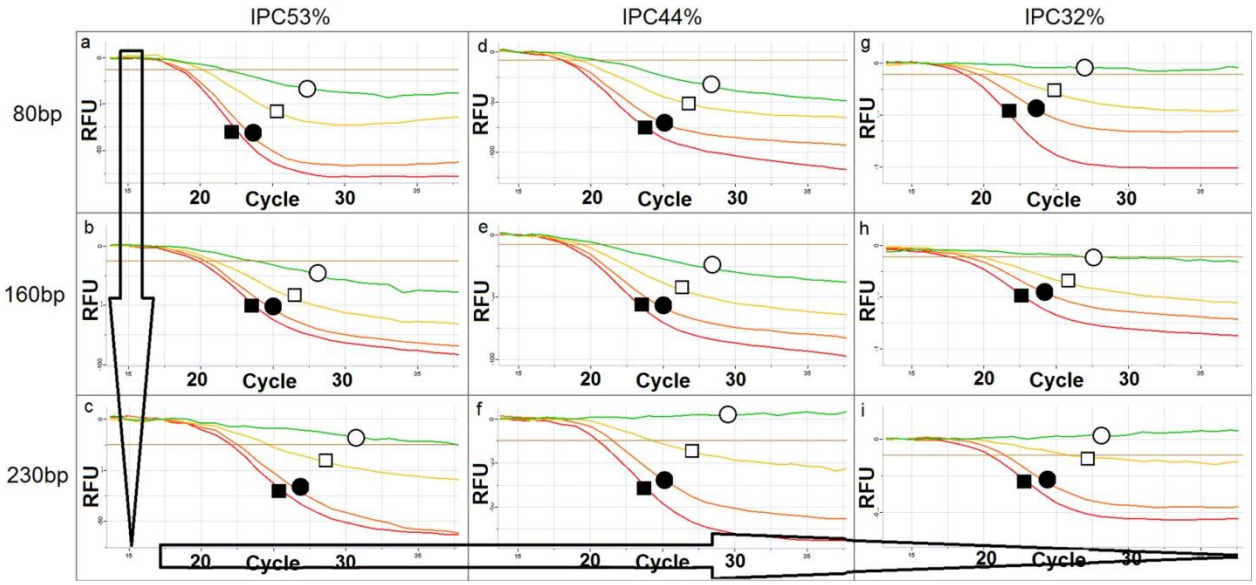

Figure 3: Combined effects of amplicon size (increasing downward) and GC content (decreasing left to right) sequence in urea at concentrations of 0 (red ■), 100 (orange ●), 300 (yellow □) and 500mM (green ○) indicating that as the amplicon size increases and as the sequence %GC content decreases, the DNA's sensitivity to inhibition can increase. Arrows indicate increasing size and decreasing GC content.

Examining amplification efficiency across all of the IPC sequences and amplicon sizes for the example of urea, (Figure 3) we find that as amplicon size increases, and amplicon GC content decreases, inhibitory effects become more detectable.

This document is a research report submitted to the U.S. Department of Justice. This report has not been published by the Department. Opinions or points of view expressed are those of the author(s) and do not necessarily reflect the official position or policies of the U.S. Department of Justice.

% Efficiency	Bile salts	Collagen	Guanidinium	Hematin	Humic Acid	Melanin	Tannic Acid	Urea
	1.0ng/µL	100ng/µL	4.5ng/µL	60uM	40ng/µL	16ng/µL	11.25ng/µL	300mM
Autosomal	**92.4±1.2%**	**87.7±1.0%**	**85.4±0.3%**	**63.5±1.7%**	**57.6±1.9%**	**62.6±2.4%**	**67.8±1.9%**	**53.3±1.7%**
Y	80.9±2.8%	**41.5±4.6%**	**42.0±3.0%**	**10.1±1.9%**	**21.1±2.4%**	**39.6±1.8%**	**33.0±0.2%**	**47.9±4.6%**
53% GC 80bp	93.1±1.8%	**82.9±0.3%**	**71.7±1.5%**	**67.8±2.9%**	**62.2±1.6%**	**72.5±1.9%**	**63.6±5.4%**	**66.1±1.1%**
53% GC 160bp	**69.2±0.6%**	**23.3±2.4%**	**61.1±1.5%**	**70.3±1.3%**	**61.5±8.9%**	**66.2±1.8%**	**61.0±3.2%**	**71.3±0.9%**
53% GC 230bp	**10.9±1.8%**	**14.0±3.8%**	**61.9±4.0%**	**51.1±0.8%**	**58.3±3.6%**	**54.6±2.1%**	**52.8±0.2%**	**65.6±2.4%**
44% GC 80bp	**88.0±0.2%**	**84.0±1.6%**	**75.1±1.0%**	**64.7±0.8%**	***51.3±3.3%***	**66.9±1.6%**	**75.5±3.9%**	**71.7±1.7%**
44% GC 160bp	**48.1±1.9%**	**48.9±3.8%**	**59.5±1.6%**	**59.5±2.8%**	**53.9±4.2%**	**66.0±0.8%**	**60.9±0.8%**	**68.2±2.4%**
44% GC 230bp	**12.9±3.3%**	***10.3±3.9%***	**63.6±0.9%**	**45.2±4.6%**	**64.9±2.3%**	***42.1±3.6%***	***50.4±1.3%***	**60.0±5.0%**
32% GC 80bp	**90.3±0.3%**	**80.2±1.9%**	**75.6±1.1%**	**55.4±0.6%**	**63.4±0.9%**	**54.7±1.9%**	**67.5±3.0%**	**60.8±3.0%**
32% GC 160bp	**75.1±0.8%**	**52.3±4.2%**	**70.7±1.1%**	**55.0±3.4%**	**58.3±1.6%**	**59.9±1.5%**	**51.8±3.9%**	**60.2±3.0%**
32% GC 230bp	***8.1±0.4%***	**34.8±2.1%**	***49.7±1.8%***	***47.0±2.5%***	**52.0±6.9%**	**54.3±3.6%**	**52.2±2.3%**	***51.4±3.2%***

Table 4: The percentage ± the observed standard error of the efficiency in the inhibited sample relative to the control sequence. All samples significantly decreased in efficiency with the addition of any PCR inhibitor, where $p<0.05$. Italicized, highlighted samples indicate the amplicon most affected by the presence of the inhibitor. In all cases, the control sequence was assumed to be 100% efficient.

Table 4 demonstrates the results across a range on inhibitors at different GC content and length.

The results show that in general, the use of a long, low GC content DNA amplicon as an internal PCR control will generally provide an increased ability to detect inhibition during the real time PCR quantification step. Furthermore, our results suggest that it should be possible to tailor the composition of IPCs in quantification kits to a desired level of sensitivity by altering the length of the internal control sequences.

Conclusions

The results from these experiments help to clarify the role of PCR inhibitors in PCR amplification and their effects on STR amplification. We see three basic types of inhibitors: DNA binding, polymerase binding and mixed mode (inhibitors which affect both polymerase and template) We note that real time

This document is a research report submitted to the U.S. Department of Justice. This report has not been published by the Department. Opinions or points of view expressed are those of the author(s) and do not necessarily reflect the official position or policies of the U.S. Department of Justice.

PCR amplification efficiency and melt curves help to elucidate the modes of inhibition and have some predictive power in defining downstream allele dropout. Furthermore we note that while allele sequence has an effect on sensitivity to PCR inhibition, the length of the amplicon is most important. Overall we find that PCR inhibition is a complex process that cannot be modeled by one specific compound. Individuals interested in validating new forensic methods should carefully chose a range of inhibitors to encompass the range of modes of inhibition. . The data on size and sequence of control DNA indicates the important effect of amplicon length on PCR inhibition. Designers of real time PCR kits who wish to optimize the length and size of their internal control sequences can utilize this data to develop better quantification kits. Lastly the results comparing the effects of different classes of inhibitors on the recovery of DNA can help to instruct the triers of fact on interpretation of difficult partial profiles and indicate that both degradation and inhibition can affect the recovery of larger alleles.

References

1. Guescini M, Sisti D, Rocchi M., Stocchi L, Stocchi V. A new real-time PCR method to overcome significant quantitative inaccuracy due to slight amplification inhibition, BMC Bioinformatics 2008;9:326:1-12
2. Weibull, W. A statistical distribution function of wide applicability. J. Appl. Mech.1951;18:293–6
3. Opel K, Chung D, McCord BR. A study of PCR inhibition mechanisms using real-time PCR. J. Forensic Sci. 2010;55(1):25-33.
4. Funes-Huacca ME, Opel K, Thompson R, McCord BR. A comparison of the effects of PCR inhibition in quantitative PCR and forensic STR analysis. Electrophoresis 2011;32(9):1084-9.

This document is a research report submitted to the U.S. Department of Justice. This report has not been published by the Department. Opinions or points of view expressed are those of the author(s) and do not necessarily reflect the official position or policies of the U.S. Department of Justice.

Full Report

Part 1: An investigation of PCR inhibition using Plexor® based quantitative PCR and short tandem repeat amplification

A common problem in forensic genetic analysis is the presence of PCR inhibitors. Inhibitors are chemical and biological matrix interferences that coextract with DNA and affect downstream processing. These interfering substances present a challenge for forensic human identification due to inhibitory effects on short tandem repeat (STR) amplification that include poor peak balance, locus-specific drop-out, enhanced stutter, and poor sensitivity. The overall result can be no amplified product or partial profiles that are difficult to interpret (1). PCR inhibitors may be introduced at any stage prior to amplification of the sample. Potential sources for inhibition include humic and tannic acids in soil, calcium and collagen in bone and tissue, hematin in blood, bile salts and catabolic substances in feces and urine, and melanin in hair. In addition, chemical components such as urea, phenol, and transition metal ions may enter during the extraction process through inadvertent contamination (1-4). Whatever the source, once present in a DNA sample, inhibitors can prevent or reduce the efficiency of PCR amplifications. This paper utilizes real-time PCR amplification to monitor changes in efficiencies and melt curves of known PCR inhibitors. Our goal in monitoring these effects, is to better understand PCR inhibition mechanisms and provide information on inhibitory mechanisms to forensic analysts, permitting them to better interpret results.

Real-time PCR – or quantitative PCR (qPCR) – is an important analytical method for determining the quantity of recovered DNA in forensic samples because of its sensitivity, specificity, and ease of automation (5). Typically in real-time PCR amplification, a fluorescent dye is introduced during thermal cycling, causing a change in fluorescent output as the double stranded DNA (dsDNA) product accumulates (6). During amplification, the number of cycles required to reach a significant change in fluorescence is known as the cycle threshold (C_T), and is determined by a linear relationship between the log of the concentration of DNA template and the number of PCR cycles (7).

This document is a research report submitted to the U.S. Department of Justice. This report has not been published by the Department. Opinions or points of view expressed are those of the author(s) and do not necessarily reflect the official position or policies of the U.S. Department of Justice.

There are different approaches that can be used for fluorescence-based detection assays including TaqMan® and Scorpion probes, SYBR Green intercalation, and the Plexor® HY System (Promega Corporation, Madison WI) (6,8-9). While the result of TaqMan and SYBR Green analysis is an increase in fluorescence intensity that is proportional to the amount of amplicon produced, the Plexor® HY system due to its quenching mechanism, produces a loss in signal as the product accumulates. Unlike other qPCR assays which involve probes or intercalating dyes, Plexor® HY does not interfere with or bind to the incipient DNA duplex since its chemistry involves quenching between two labeled nucleotides, isoguanine (iso-dG) and 5'-methylisocytosine (iso-dC) at the distal end of the amplicon (10). The reaction involves the use of a fluorescently labeled iso-dC on the 5' end of one of the two primers. During the amplification process, iso-dG, containing the quencher, is specifically incorporated at a position complementary to the iso-dC in the opposite strand. Once this occurs, a reduction in the fluorescent signal occurs that is proportional to the quantity of dsDNA.

Since quenched amplicons produce a significant change in fluorescent signal as they are denatured, a melt curve can be produced at the end of the amplification cycle that is characteristic of the PCR product. The melting temperature (T_m) can be used to confirm that the amplified product is from the intended target DNA and contains the appropriate product length, sequence, and strand complementarity (11). In addition, nonspecific amplification products such as primer-dimer artifacts, mis-priming, and DNA inhibition will result in alterations to the melting temperature and curve. For example, PCR inhibitors that bind DNA will result in reproducible shifts in the melt curve (12). In addition, this type of PCR inhibition can be identified based on a shift in C_T when compared to uninhibited samples. To do this, an internal (non-human) positive control sequence (IPC) is added to the real-time reaction mixture and the relative differences between the amplification of this control sequence in an unknown sample and a DNA standard are assessed. The presence of a PCR inhibitor in the reaction mixture will produce a higher C_T value (9,13).

An alternative mechanism for PCR inhibition is to alter the efficiency (theoretical doubling) of *Taq* polymerase. *Taq* polymerase inhibition can be recognized by a change in the slope of the exponential

This document is a research report submitted to the U.S. Department of Justice. This report has not been published by the Department. Opinions or points of view expressed are those of the author(s) and do not necessarily reflect the official position or policies of the U.S. Department of Justice.

curve produced by the real-time amplification. There is also a minor effect on the C_T value but this is the result of the change in slope and not a reduction in template availability (12). *Taq* polymerase inhibition has been modeled using parameters based on a Richards function as has been discussed by Guescini et al. (14,15). The most common effect of any inhibitor is unsuccessful genotyping, which result in either no STR profiles or partial profiles that are difficult to interpret. Inhibitors that affect *Taq* polymerase efficiency generally result in a generic loss of the larger loci. This may be the result of a slower base incorporation rate in the presence of inhibition. Inhibitors that bind DNA can also show locus-specific effects, resulting in a pattern of allele loss in which some loci are affected and others are not (16). This is presumably due to a preference of the inhibitor to bind specific sections of the template and not others.

Experimentally, there are several approaches ranging from dilution to magnetic bead extraction that can result in some success in overcoming the effects of inhibition (17,18). However, many of these cleanup methods involve wash steps which may affect recovery of the template DNA, making them undesirable for samples containing low levels of DNA. Newer PCR multiplex kits have also been shown to be effective in reducing inhibition due to improved buffer formulations. However, these kits are still affected by inhibitors at higher concentrations (19,20). Thus it is important to understand and identify the mechanisms of inhibition, in order to better interpret results obtained from such samples. This study will examine the effects of a variety of PCR inhibitors using the Plexor® HY qPCR assay while monitoring amplification efficiency and slope, C_T, and melt curves of eleven inhibitors known to affect forensic samples. These included calcium, humic acid, collagen, phenol, tannic acid, hematin, bile salts, melanin, EDTA, urea and guanidinium thiocyanate.

Materials and Methods

DNA Standards and Stock Solution

The Plexor® HY Male Genomic DNA Standard, provided with the Plexor® HY System, was used to generate standard curves ranging from 50 ng/µL to 3.2 pg/µL. For inhibition tests, multiple buccal swabs were collected from a human male individual. The swabs were extracted using an organic

This document is a research report submitted to the U.S. Department of Justice. This report has not been published by the Department. Opinions or points of view expressed are those of the author(s) and do not necessarily reflect the official position or policies of the U.S. Department of Justice.

(phenol/chloroform/isomyl alcohol (PCIA) [Sigma Aldrich, St. Louis, MO]) extraction protocol (21). The extracts were combined into one stock solution, quantified using the protocol in the Plexor® HY Systems Technical Manual (22), and diluted to approximately 2 ng/µL concentration.

Real-Time PCR Analysis

Testing of the Plexor® HY System on extracted samples was performed on the Corbett Rotorgene 6000 Real-Time PCR System (Qiagen Inc., Valencia, CA). Plexor® HY reaction mixture includes primer sets for autosomal, Y, and internal positive control (IPC) sequences. For the purposes of this study, the autosomal results were mainly monitored to simplify analysis, however in certain cases sequence differences between the different amplicons caused effects that were seen and noted below. The real-time reaction conditions were based on the Plexor® HY Systems Technical Manual (22) with 1 µL of nuclease-free water substituted with inhibitor. DNA concentration of 2 ng/µL was added to the PCR reaction mixture before separating the mixture into aliquots and adding the inhibitor. The final reaction volume was 20 µL. Cycling parameters for the reactions were as follows: hold for 2 minutes at 95 °C; 40 cycles of 95 °C for 10 seconds, then 60 °C for 20 seconds with data collection during the elongation/extension step. The melt cycle was: ramp from 65 °C to 92 °C, 0.5 °C for each step, with a 90 second pre-melt and 5 seconds for each temperature step. All reactions were performed in triplicate.

Inhibitor Preparations

The inhibitor stock solutions were prepared as follows: calcium hydrogen phosphate (Aldrich, Milwaukee, WI), 100 mM in 0.5 N hydrochloric acid (Fisher Scientific, Waltham, MA); humic acid (Alfa Aesar, Ward Hill, MA), 1 mg/mL in water; collagen (from calf skin) (Sigma), 1 mg/mL in 0.1 N acetic acid (Fisher Scientific); phenol solution (Sigma), 100 mM in water; tannic acid (Sigma), 1 mg/mL in water; hematin (ICN Biomedicals, Aurora, OH), 100 mM in 0.1 N sodium hydroxide (Fisher Scientific); melanin (Sigma), 1mg/mL in 0.5 N ammonium hydroxide (Fisher Scientific); urea (Fisher Scientific), 10 M in water; bile salts (sodium cholate plus deoxycholate) (Fluka, St. Louis, MO), 100 mg/mL in water;

This document is a research report submitted to the U.S. Department of Justice. This report has not been published by the Department. Opinions or points of view expressed are those of the author(s) and do not necessarily reflect the official position or policies of the U.S. Department of Justice.

EDTA (Fluka), 0.5 M in water; Guanidinium thiocyanate (Sigma), 100 mg/mL in water. All subsequent dilutions were prepared with water. These inhibitors were added to samples prior to quantification and STR analyses.

Inhibitor Concentrations

A range of concentrations was tested to determine the inhibitor concentration at which a change in the signal output would be observed. The starting concentrations were based on previous work with these inhibitors (12) and information on their chemical properties. The qPCR tests were conducted using Plexor® HY multiplex primers (22). The ranges of concentrations for each inhibitor are presented in Table 1.

TABLE 1- Summary of Real-Time PCR inhibition results

Inhibitor	**Concentration**	**C_T shift Range (cycles)**	**T_m shift range (°C)**	**Plexor® mode of inhibition**
Calcium	0, 0.5, 1.0 1.5, 2.0, 2.5 mM	25 - 37	80.4	*Taq* polymerase inhibitor
Tannic Acid	0, 5, 10, 15, 17.5, 20. 22.5 ng/µL	25 - 37	80.5 - 80.4	*Taq* polymerase inhibitor
Bile Salts	0, 0.25, 0.50, 0.75, 1.00, 1.25, 1.50 µg/µL	25 - 36	80.5 - 80.0	DNA binding inhibitor
Humic Acid	0, 5, 10, 15, 20, 25, 30 ng/µL	25 - 36	80.5 - 80.2	DNA binding inhibitor
Hematin	0, 15, 30, 45, 60, 75, 90, 105 µM	25 - 36	80.5 - 79.4	DNA binding inhibitor
Melanin	0, 10, 20, 30, 40, 50, 60 µg/µL	25 - 34	80.5 - 79.4	DNA binding inhibitor
EDTA	0, 0.4, 0.8, 1.2, 1.6, 2.0, 2.4 mM	25 - 34	80.5 - 78.2	DNA binding inhibitor
Phenol	0, 33, 66, 83, 100, 116, 133 µg/µL	25 - 30	80.5 - 79.1	Mixed mode inhibitor
Collagen	0, 25, 38, 50, 63, 75, 88, 100 ng/µL	25 - 30	80.7 - 84.3	Mixed mode inhibitor
Urea	0, 200, 400, 600, 800, 1000, 1200 mM	25 - 29	80.5 - 79.4	Mixed mode inhibitor
Guanidinium	0, 1.5, 3.0, 4.5, 6.0, 7.5, 9.0 µg/µL	25 - 28	80.6 - 83.5	Mixed mode inhibitor

This document is a research report submitted to the U.S. Department of Justice. This report has not been published by the Department. Opinions or points of view expressed are those of the author(s) and do not necessarily reflect the official position or policies of the U.S. Department of Justice.

Data Analysis

Following data collection on the real-time instrument, raw data were exported from the instrument software and imported into the Plexor® Analysis Software version 1.5.4.18 (Promega Corporation, Madison WI). The software generated the amplification and melt curves, cycle threshold (C_T), product melt temperature (T_m), standard curve and unknown sample quantification data. For qPCR amplification, four parameters were used to classify PCR inhibition: efficiency, cycle threshold, melt curve and final concentration.

The efficiency reveals the dynamics of the PCR reaction for each sample, which includes reaction components, potential presence of inhibitors and cycling parameters. A more efficient amplification will generate more products with fewer cycles. The individual PCR efficiency is expressed as a numerical value (between 1 and 2) and is calculated from the slope of the amplification curve in the exponential phase ($E = 10^{slope}$) (23). An ideal PCR efficiency is 100% or E=2, which means that the amount of amplicon has doubled; therefore E=1 means that there is no amplification. Efficiencies were initially obtained by exporting the raw Excel data from the Real-Time PCR System and importing into LinRegPCR (23), a program that identifies the exponential phase of the reaction by plotting the fluorescence on a log scale. Then a linear regression is performed at the tangent to the curve, leading to the estimation of the efficiency of each PCR reaction (24). A more complete modeling of the overall PCR reaction was also performed by modeling the entire slope of the PCR reaction using the program Curve Expert (http://www.curveexpert.net). Real-time PCR reactions were modeled using the Weibull fit parameters contained in this program. $y = a - b*\exp(-cx^d)$.

Cycle threshold (C_T) values are inversely proportional to the log of the initial template DNA concentration. As a result, a higher C_T value generally corresponds to a lower amount of template DNA. Plexor® Analysis Software was used to determine C_T based on noise levels and was set by default at 10 standard deviations above the mean baseline fluorescence (22).

In addition to the efficiency and C_T values, melt curve shifts resulting from variations in T_m were monitored as well as final product concentration. The STR allele peak heights, heterozygous peak

This document is a research report submitted to the U.S. Department of Justice. This report has not been published by the Department. Opinions or points of view expressed are those of the author(s) and do not necessarily reflect the official position or policies of the U.S. Department of Justice.

balance, and the presence of allele drop-out were also examined (see below).

STR Analysis

0.5ng DNA along with appropriate amounts of inhibitors were added to a 25 µL reaction and amplified as described in the PowerPlex ® 16 System (Promega, 2008) and PowerPlex ® 16 HS System (25) Technical Manuals. Due to differences in response to inhibition between the STR kits and real time PCR, inhibitor concentrations were sometimes increased when performing STR analysis, Figures 13-15, Table 2. After amplification, samples were prepared by combining 1 µL of sample, 9.5 µL of Hi-Di™ formamide and 0.5 µL of Internal Lane Standard 600 (ILS600) per reaction. Separation and detection of STR amplification products were performed on an ABI Prism® 310 Genetic Analyzer (Applied Biosystems) using the *GS STR POP4 (1mL) A* module. Samples were injected at 15 kV for 5 seconds with 15 kV separation at 65 °C and a run time of 35 minutes. Data analysis was performed using the GeneMapper Software version 4.0 (Applied Biosystems). Electropherograms were interpreted based on peak height and allele drop-out at particular loci when compared to the control with a minimum detection threshold of 50 RFUs.

TABLE 2- Summary of inhibition results

Inhibitor	**Plexor® Mode of Inhibition**	**Final Concentration at 50% qPCR Inhibition**	**Final Concentration at 50% Drop-out of 1ST allele (qPCR Concentration)**	**Drop-out or Decreased Intensity: Loci below 250 bp**	**Drop-out or Decreased Intensity: Loci above 250 bp**
Calcium	*Taq*	1.0 mM	0.8 mM (1.0 mM)	Am, vWA, D21, D8	TPOX, FGA
Tannic Acid	*Taq*	15 ng/µL	32 ng/µL (25.6 ng/µL)	Am, vWA	D16, D18, PE, CSF, PD, TPOX, FGA
Bile Salts	DNA	1.25 µg/µL	1.2 µg/µL (1.0 µg/µL)	Am, D13, D8	D16, D18, PE, CSF, PD, TPOX, FGA
Humic Acid	DNA	20 ng/µL	8 ng/µL (6.4 ng/µL)	Am, vWA, D21, D8	PD, TPOX, FGA
Hematin	DNA	60 µM	48 µM (38.5 µM)	Am, vWA, D8	D16, D18, CSF, PD,

This document is a research report submitted to the U.S. Department of Justice. This report has not been published by the Department. Opinions or points of view expressed are those of the author(s) and do not necessarily reflect the official position or policies of the U.S. Department of Justice.

					TPOX
Melanin	DNA	40 µg/µL	32 ng/µL (25.6 ng/µL)	D13, D8	D16, D18, CSF, PD
EDTA	DNA	1.2 mM	0.6 mM (0.5 mM)	Am, D3, D5, vWA, D13, D8,	D16, D18, PE, CSF, PD, TPOX, FGA
Phenol	DNA/Taq	100 µg/µL	52 µg/µL (41.6 µg/µL)	Am, D3, D5, vWA, D13, D8, D7	D16, D18, PE, CSF, PD, TPOX, FGA
Collagen	DNA/*Taq*	100 ng/µL	200 ng/µL (160 ng/µL)	N/A	PD, TPOX, FGA
Urea	DNA/*Taq*	400 mM	240 mM (192 mM)	Am, D13, D8	D16, D18, PE, CSF, PD, TPOX, FGA
Guanidinium	DNA/*Taq*	7.5 µg/µL	7.2 µg/µL (5.8 µg/µL)	D3, D13, D21, D7	D16, D18, PE, CSF, PD, TPOX, FGA

Abbreviations: Am: Amelogenin, PE: Penta E, D18: D18S51, D2: D21S11, D3: D3S1358, D8: D8S1179, PD: Penta D, CSF: CSF1PO, D16: D16S539, D7:D7S820, D13: D13S317 and D5: D5S818.

Note: PowerPlex® 16 HS and Plexor® HY final concentrations vary because they are based on a 25 µL and 20 µL reaction volume respectively.

Results

PCR inhibitors found in DNA samples can affect real-time PCR results as well as the quality and interpretation of downstream STR data. Inhibitory effects on qPCR amplification were identified by changes in the slope of the exponential amplification curves, amplification efficiency, C_T values, and changes in T_m as revealed in the melt curves. Our hypothesis was that inhibitors can be classified based on their mechanism of action. Those mainly binding to DNA should produce shifts in the melt curves and changes in C_T while those mainly affecting the *Taq* polymerase should produce changes in efficiency and exponential slope of the PCR amplification curve (12,55). The different responses to inhibition are demonstrated in Figure 1. Exponential slopes do not change with inhibitors that bind DNA (Figure 1A) while inhibitors that primarily affect *Taq* polymerase produce exponential PCR curves that radiate out

This document is a research report submitted to the U.S. Department of Justice. This report has not been published by the Department. Opinions or points of view expressed are those of the author(s) and do not necessarily reflect the official position or policies of the U.S. Department of Justice.

from a single point (Figure 1B). Mixed mode inhibition can also exist. In this study, the effects of eleven different PCR inhibitors on Plexor® HY qPCR data were examined and the results are summarized in Table 2. The table includes PCR inhibition over a wide range of concentrations, where an approximate 50% loss in amplification efficiency occurs and the concentration at which at least the loss of at least one allele occurred 50% of the time.

Calcium

Calcium is the main inorganic component of bone, which is two-thirds of the composition (26). The results obtained when increasing concentrations of calcium were added to the PCR reaction mixture included low amplification efficiencies at concentrations of 1.5 mM and higher, a delay in C_T and no changes in the T_m (Figure 1). A close examination of the data in Figure 1 reveals that as the concentration of inhibitor increases, the slope of the exponential portion of the PCR curve decreases. The changes in C_T seen at concentrations of 1.0 mM and higher are therefore mainly due to slope changes and are not a result of reduction in the availability of template. Thus the mechanism of inhibition is likely to be an interference with the interaction between the polymerase enzyme and magnesium, which acts as a cofactor. Calcium and magnesium are both divalent cations and therefore similar in structure and properties, so they may compete with one another during the PCR amplification. These results suggest that calcium is a *Taq* polymerase inhibitor.

This document is a research report submitted to the U.S. Department of Justice. This report has not been published by the Department. Opinions or points of view expressed are those of the author(s) and do not necessarily reflect the official position or policies of the U.S. Department of Justice.

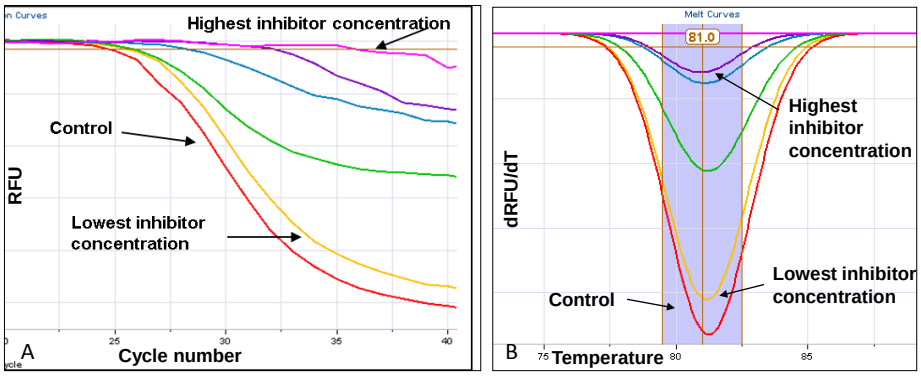

calcium

Figure 1: A. Changes in Autosomal Plexor® HY amplification (left) and B. melt curves (right) at the following concentrations of calcium: 0mM (red), 0.5 mM (yellow), 1.0 mM (green), 1.5 mM (blue), 2.0 mM (purple), 2.5 mM (pink).

Humic Acid

Humic acid is one of the major constituents of soil organic matter and consists of a mixture of decomposed plant and animal residue (27). The results obtained when humic acid was added at increasing concentrations to the PCR reaction mixture included a slight reduction in efficiency of the amplification at concentrations of 25 ng/µL and higher and increasing C_T values. This indicated that inhibition was more due to humic acid binding to DNA than the interference with *Taq* polymerase (Figure 2A). This was consistent with previous results that indicated inhibitor binding to DNA when utilizing SYBR green at high concentrations of humic acid (12). However, results did not produce significant changes in the melt curve, which conflicted with inhibitor binding to DNA effects (Figure 2B). Humic acid is a relatively large molecule and could be a possible DNA intercalator or groove binder due to its flat planar system as well as its size, which accommodates wrapping around the DNA (27-29). An inhibitor of that size may

This document is a research report submitted to the U.S. Department of Justice. This report has not been published by the Department. Opinions or points of view expressed are those of the author(s) and do not necessarily reflect the official position or policies of the U.S. Department of Justice.

not bind well to very short amplicon lengths (<200 bp), which may explain the relative lack of melt curve effects in this assay. These results suggest the mechanism of inhibition for humic acid is likely to be an affect on the availability of DNA template but this result is not well corroborated by melt curve effects.

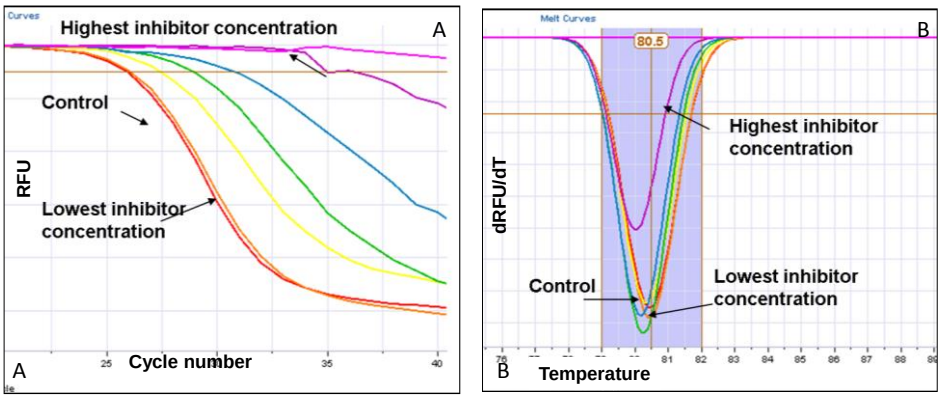

Humic acid

Figure 2: A. Changes in Autosomal Plexor® HY amplification (left) and B. melt curves (right) at the following concentrations of humic acid: 0 ng/µL (red), 5 ng/µL (orange), 10 ng/µL (yellow), 15 ng/µL (green), 20 ng/µL (blue), 25 ng/µL (purple), 30 ng/µL (pink).

Collagen

Collagen is a protein that constitutes the bulk of the organic portion of bone and is a major component in connective tissue (30). The results obtained when increasing concentrations of collagen were added to the PCR reaction mixture included a reduction in the amplification efficiency at concentrations of 62.5 ng/µL and greater, and a 4 cycle C_T shift occurred along with a 4° shift in the T_m (Figure 3). A C_T increase along with a gradual change in slope of the amplification curve suggests an effect on amplification efficiency more than the blocking of available template. The T_m increased as inhibitor concentration increased, which signifies that collagen prevents denaturing of the dsDNA and may be interfering through hydrogen bonding. In aqueous solution, a collagen-DNA aggregate leads to

This document is a research report submitted to the U.S. Department of Justice. This report has not been published by the Department. Opinions or points of view expressed are those of the author(s) and do not necessarily reflect the official position or policies of the U.S. Department of Justice.

the destruction of the collagen triple helix and stabilization of the DNA double helix structure due to its hydrogen-bonding network (31-32). The structure of collagen could allow possible groove binding and wrapping throughout the DNA molecule. These results suggest that the mechanism of inhibition for collagen is mixed mode, ie. binding DNA as well as inhibiting *Taq* polymerase.

Interestingly, the effect on the IPC was minimal except at the highest levels of inhibitor (results not shown). The IPC is a non-human sequence which is added to the real-time reaction mixture to detect problems with amplification that are not related to template concentration. If no template is present, the IPC will still amplify. Conversely, if inhibition is present, the IPC will amplify poorly regardless of template concentration. Thus because collagen inhibition affects the IPC amplification far less than that for the autosomal DNA locus, sequence-specific binding of the inhibitor may be occurring, since the two amplicons are of similar size (99 and 130bp). Because the IPC is the main tool used to detect PCR inhibition, the analyst might incorrectly conclude that inhibition was absent.

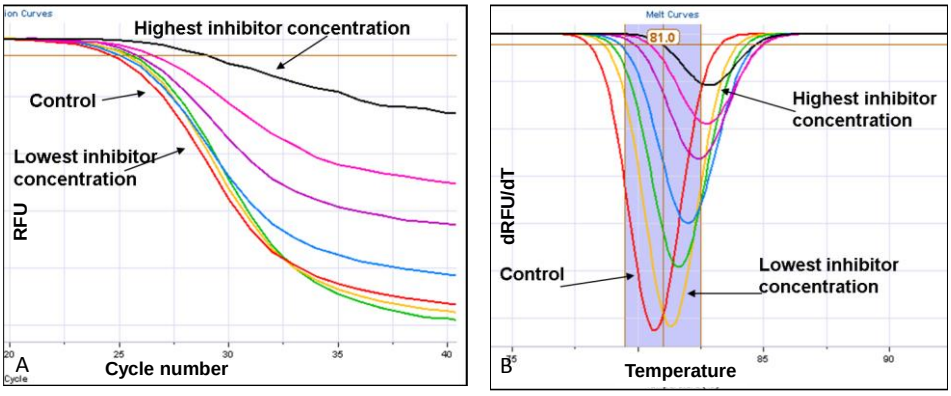

collagen

Figure 3: Changes in Autosomal Plexor® HY amplification (left) and melt curves (right) at the following concentrations of collagen: 0 ng/µL (red), 25 ng/µL (orange), 37.5 ng/µL (yellow), 50 g/µL (green), 62.5 ng/µL (blue), 75 ng/µL (purple), 87.5 ng/µL (pink), 100 ng/µL (black).

This document is a research report submitted to the U.S. Department of Justice. This report has not been published by the Department. Opinions or points of view expressed are those of the author(s) and do not necessarily reflect the official position or policies of the U.S. Department of Justice.

Phenol

Phenol is a highly reactive organic compound and can be present in samples that have been extracted using PCIA. The results obtained when increasing concentrations of phenol were added to the PCR reaction mixture included a reduction in amplification efficiency and a 2 cycle shift in C_T, indicating *Taq* polymerase inhibition and inhibitor binding to DNA respectively (Figure 4A). Changes in the melt curve by approximately 3°C also showed evidence of inhibitor binding to DNA (Figure 4B). Like collagen, the mechanism of inhibition is likely to include effects of the inhibitor on the polymerase as well as binding to the DNA. Although phenol is a protein denaturant, it may still promote unzipping of DNA through hydrogen bonding to single stranded DNA (33). Phenol binding to DNA results in a decrease in T_m, which indicates a weakening of the hydrogen bonds between bases and an enhancement in the denaturation process. Traces of phenol can completely inactivate the *Taq* polymerase (34, 35).

Figure 4: Changes in Autosomal Plexor® HY amplification (left) and melt curves (right) at the following concentrations of phenol: 0 µg/µL (red), 33 µg/µL (orange), 66 µg/µL (yellow), 83 µg/µL (green), 100 µg/µL (blue), 116 µg/µL (purple), 133 µg/µL (pink).

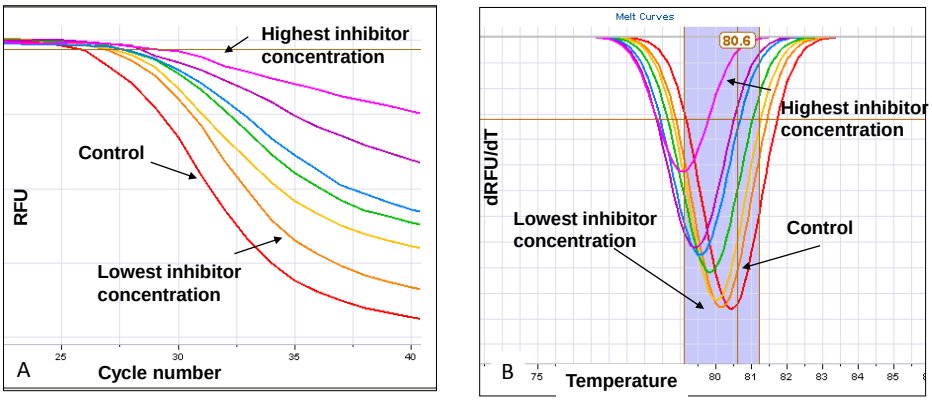

phenol

This document is a research report submitted to the U.S. Department of Justice. This report has not been published by the Department. Opinions or points of view expressed are those of the author(s) and do not necessarily reflect the official position or policies of the U.S. Department of Justice.

Tannic acid

Tannic acid is a natural component of some types of wood and other plant material as well as a color agent found in leather (2). The results obtained when increasing concentrations of tannic acid were added to the amplification mixture included a gradual change in the slope of the amplification curves, minimal changes in C_T, insignificant changes in T_m and a reduction of efficiency at higher concentrations of inhibitor (Figure 5). Tannic acid contains a large number of electronegative groups and could be chelating the magnesium, inactivating the *Taq* polymerase. This would explain Plexor® HY results with efficiency loss. For example, free phenolic groups in tannic acid oxidize to form quinones that covalently bond and inactivate the *Taq* polymerase (24). These results suggest the mechanism of inhibition for tannic acid is likely to be *Taq* polymerase inhibition.

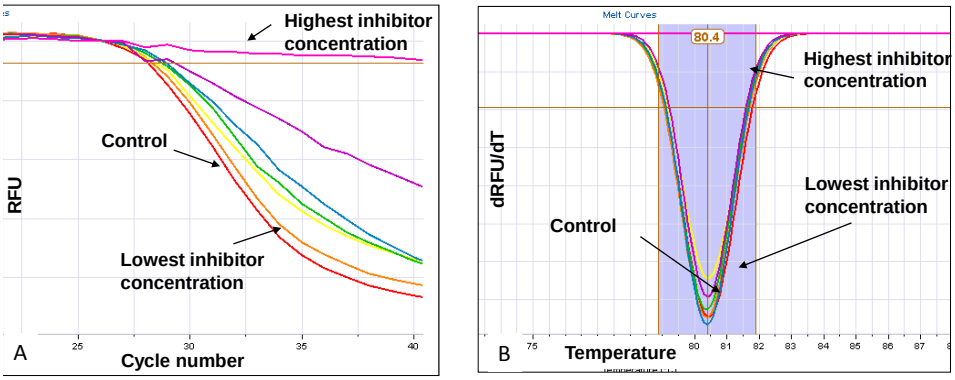

Tannic acid

Figure 5: A. Changes in Autosomal Plexor® HY amplification (left) and B. melt curves (right) at the following concentrations of tannic acid: 0 ng/µL (red), 5 ng/µL (orange), 10 ng/µL (yellow), 15 ng/µL (green), 17.5 ng/µL (blue), 20 ng/µL (purple), 22.5 ng/µL (pink).

This document is a research report submitted to the U.S. Department of Justice. This report has not been published by the Department. Opinions or points of view expressed are those of the author(s) and do not necessarily reflect the official position or policies of the U.S. Department of Justice.

Hematin

Hematin is a metal chelating molecule found in red blood cells (36). The results obtained when increasing concentrations of hematin were added to the amplification mixture included an increase in C_T that appeared to be related to a loss of template (Figure 6A). There was also a significant reduction in amplification efficiency at concentrations of 60 µM and higher (Figure 6A). Like phenol, hematin showed a 3° decrease in T_m (Figure 6B). While the porphyrin structure of hematin may allow chelation with the magnesium ions, producing the efficiency changes, we did not see a strong effect (36). Thus the mechanism of inhibition for hematin is likely to be binding to DNA.

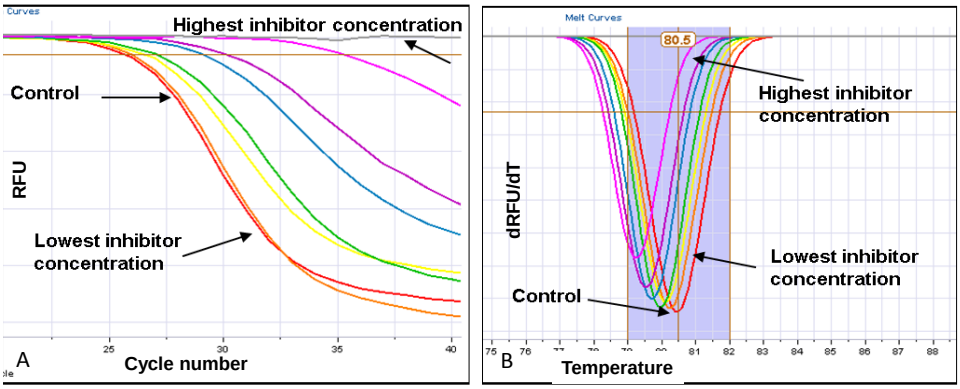

hematin

Figure 6: Changes in Autosomal Plexor® HY amplification (left) and melt curves (right) at the following concentrations of hematin: 0 µM (red), 15 µM (orange), 30 µM (yellow), 45 µM (green), 60 µM (blue), 75 µM (purple), 90 µM (pink), 105 µM (grey).

Melanin

Melanin is a pigment found in human hair and skin, and is a possible inhibitor for telogen hair samples (37). The results obtained when increasing concentrations of melanin were added to the amplification mixture included a 10 cycle increase in C_T for amplification curves, minimal changes in

This document is a research report submitted to the U.S. Department of Justice. This report has not been published by the Department. Opinions or points of view expressed are those of the author(s) and do not necessarily reflect the official position or policies of the U.S. Department of Justice.

PCR efficiency and a decrease in T_m (Figure 7). These results were consistent with a loss of available template. Studies support the theory that bacterial melanin interacts with DNA by intercalating between the basepairs of DNA (38). Other studies have shown reversible binding between melanin and a thermostable DNA polymerase, which inevitably restores the activity of the enzyme (39). However, these results, and melanin results from previous inhibition studies (12), indicate that the mechanism of inhibition is likely to be melanin binding DNA.

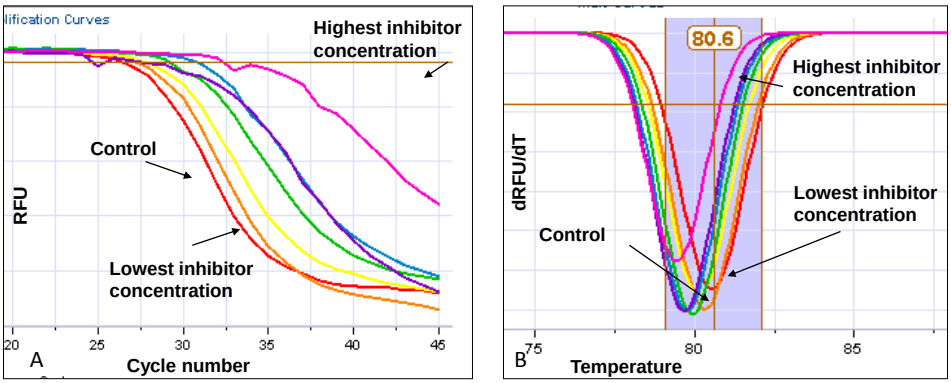

melanin

Figure 7: Changes in Autosomal Plexor® HY amplification (left) and melt curves (right) at the following concentrations of melanin: 0 µg/µL (red), 10 µg/µL (orange), 20 µg/µL (yellow), 30 µg/µL (green), 40 µg/µL (blue), 50 µg/µL (purple), 60 µg/µL (pink).

Bile salts

Bile salts are a group of PCR inhibitors present in feces (1, 40). The results obtained when increasing concentrations of bile salts were added to the PCR reaction mixture included minor effects on

This document is a research report submitted to the U.S. Department of Justice. This report has not been published by the Department. Opinions or points of view expressed are those of the author(s) and do not necessarily reflect the official position or policies of the U.S. Department of Justice.

amplification and melt curves that were similar to those from melanin - minimal loss of efficiency, a slight decrease in T_m, and a major delay in C_T values (Figure 8). Bile salts contain both polar and nonpolar regions and have been shown to inhibit bacterial growth in the small intestine due to a combination of membrane degradation and DNA damage (41). The results seen here suggest that bile salts make DNA inaccessible for the polymerase, reducing available template. The changes in the amplification and melt curves indicate that the mechanism of inhibition for bile salts is likely to be due to a reduction in the availability of DNA template.

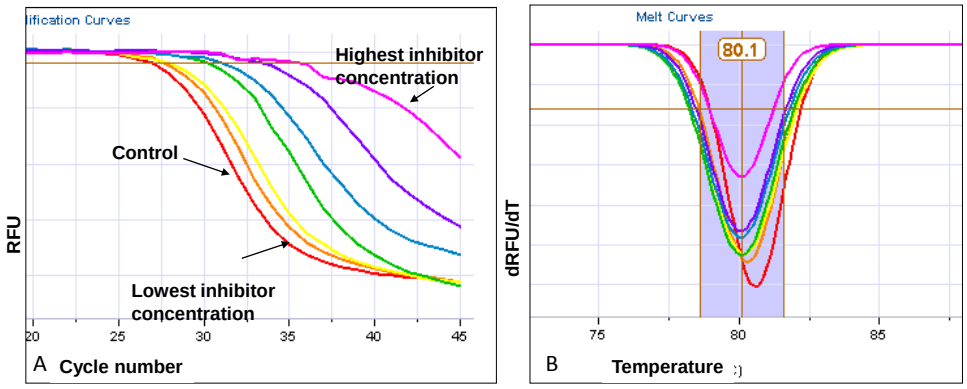

Bile salts

Figure 8: A. Changes in Autosomal Plexor® HY amplification (left) and B. melt curves (right) at the following concentrations of bile salts: 0 µg/µL (red), 0.25 µg/µL (orange), 0.5 µg/µL (yellow), 0.75 µg/µL (green), 1.0 µg/µL (blue), 1.25 µg/µL (purple), 1.5 µg/µL (pink).

Urea

Urea is the most abundant organic waste product and the major inhibitory component in urine (42). The results obtained when increasing concentrations of urea were added to the PCR reaction mixture

This document is a research report submitted to the U.S. Department of Justice. This report has not been published by the Department. Opinions or points of view expressed are those of the author(s) and do not necessarily reflect the official position or policies of the U.S. Department of Justice.

included a 4 cycle increase in C_T values that was more related to changes in the slope of the amplification curve than loss of template (Figure 9A). There was also a gradual loss of efficiency, especially those at higher concentrations of inhibitor (Figure 9A). The melt curve showed decrease in T_m of 1.5°C, indicating some binding of urea to DNA (Figure 9B). Urea is known to be a potent disruptor of non-covalent bonding and therefore may act directly on the polymerase, or it may prevent primer annealing (42). Thus the mechanism of inhibition for urea is likely to be mixed mode inhibition.

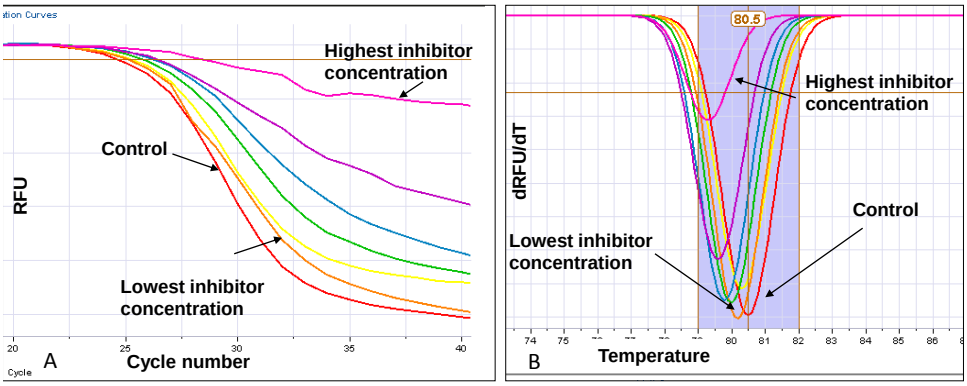

urea

Figure 9: A. Changes in Autosomal Plexor® HY amplification (left) and B. melt curves (right) at the following concentrations of urea: 0 mM (red), 100 mM (orange), 200 mM (yellow), 300 mM (green), 400 mM (blue), 500 mM (purple), 600 mM (pink).

EDTA

EDTA is a chelating agent widely used to sequester di- and trivalent metal ions (43, 44). Results obtained when increasing concentrations of EDTA were added to the PCR reaction mixture showed minimal changes in PCR reaction efficiency and significant C_T shifts related to loss of template (Figure 10A). For this inhibitor, the IPC results were different from the autosomal results, with the IPC showing far greater changes in efficiency. This is likely the result of some sequence-specific binding. A decrease

This document is a research report submitted to the U.S. Department of Justice. This report has not been published by the Department. Opinions or points of view expressed are those of the author(s) and do not necessarily reflect the official position or policies of the U.S. Department of Justice.

of approximately 3 °C was seen in the melt curve at the highest inhibitor concentration (Figure 10B). Since EDTA is a divalent cation complexing agent, it was expected to inhibit the reaction by chelating magnesium ions that are necessary for the activity of DNA polymerase. However, there was minimal effect on the amplification efficiency, thus the inhibition mechanism of EDTA may be related to its ability to inhibit DNA synthesis by affecting the stability of dsDNA (45). The concomitant rise in C_T and drop in melt temperature with increasing EDTA supports this possibility (Figure 10). These results support a conclusion that EDTA is a DNA binding inhibitor.

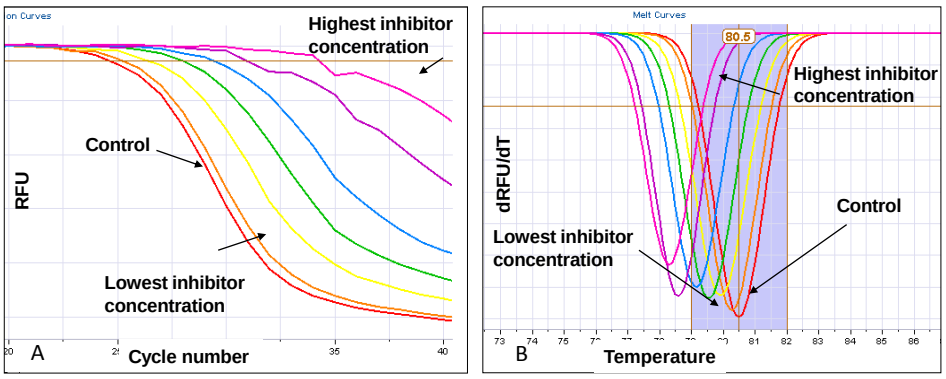

EDTA

Figure 10:A. Changes in Autosomal Plexor® HY amplification (left) and B. melt curves (right) at the following concentrations of EDTA: 0 mM (red), 0.4 mM (orange), 0.8 mM (yellow), 1.2 mM (green), 1.6 mM (blue), 2.0 mM (purple), 2.4 mM (pink).

Guanidinium

Guanidinium is commonly found in the form of guanidinium thiocyanate, a laboratory reagent used primarily for the isolation of nucleic acids (46), and other guanidinium salts. The results obtained when increasing concentrations of guanidinium were added to the PCR reaction mixture included shifts in C_T

This document is a research report submitted to the U.S. Department of Justice. This report has not been published by the Department. Opinions or points of view expressed are those of the author(s) and do not necessarily reflect the official position or policies of the U.S. Department of Justice.

which appeared to be mainly due to loss of template (Figure 11A). Guanidinium results demonstrate melt curve shifts of up to 3°C (Figure 11B). Like collagen, guanidinium increased in T_m as inhibitor concentration increased indicating binding to the DNA rather than disruption. However, the amplification efficiency values for guanidinium were low at 7.5 µg/µL. Overall, mechanism of inhibition is likely to be mixed mode with effects on *Taq* polymerase amplification efficiency as well as inhibitor binding to DNA. Interestingly, guanidinium is similar in structure to urea, both of which are denaturants. However, the melt curve results show opposing effects. This may be due to charge effects. While urea is neutral at physiological pH's, guanidinium is protonated and as a result could possibly be shielding the phosphates, keeping the structure intact instead of denaturing the DNA molecule (47). These results support a conclusion that guanadinium is a mixed mode PCR inhibitor.

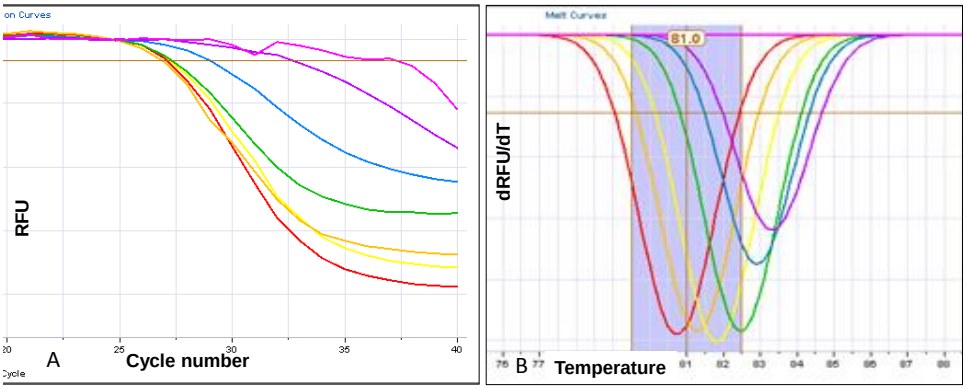

guanidinium

Figure 11: A. Changes in Autosomal Plexor® HY amplification (left) and B. melt curves (right) at the following concentrations of guanidinium: 0µg/µL (red), 1.5µg/µL (orange), 3.0µg/µL (yellow), 4.5 µg/µL (green), 6.0 µg/µL (blue), 7.5 µg/µL (purple), 9.0 µg/µL (pink).

This document is a research report submitted to the U.S. Department of Justice. This report has not been published by the Department. Opinions or points of view expressed are those of the author(s) and do not necessarily reflect the official position or policies of the U.S. Department of Justice.

Model Data Analysis

It was noted that two different processes could account for variations in C_T. In general, C_T values that increase without major changes in the slope of the exponential amplification curve may indicate inhibitor binding to DNA. However, changes in C_T associated with significant changes in the slope of the exponential curve may indicate affects associated with *Taq* polymerase processivity.

As reported by Guescini et al. (14), effects of *Taq* polymerase inhibition may be modeled using the Richards function (equation 1),

$$F_x = \frac{F_{\max}}{\left[1+e^{\left(-\frac{1}{b}(x-c)\right)}\right]^d} + F_b$$

Equation 1

where F_x = fluorescence at x cycles, b is the slope of the curve at the inflection point, c is the number of cycles at midpoint or one half of F_x, x is the cycle number, d is the Richards coefficient (related to inhibitory effects), and F_b is the background fluorescence.

Initial curve-fitting of the PCR inhibition results was performed by importing experimentally derived fluorescence data into ZunZun.com (an on-line curve fitting program) to generate the Richards function parameters (49). These results were plotted and compared to the raw excel data exported from the Rotor-Gene 6000 software. Unfortunately, it was found that the Richards Function fits failed as the sigmoidal shape of the curve was significantly modified by increasing inhibitor concentrations.

We then continued to experiment with different non-linear curve fitting models including the following; (1) the Gompertz Model y = a * exp (-exp(b - cx)), (2) the Logistic Model y = a / (1 + exp (b - cx), (3) the Morgan-Mercer-Flodin (MMF) Model $y = (ab + cx^d)/(b + x^d)$ and (4) the Weibull Model $y = a - b*\exp(-cx^d)$, using CurveExpert Professional Software (50, 51). The model that fit the data with the lowest standard error and the best comparative fit to the data curves was the Weibull model (52-54). This model is a four parameter model which has an inflection point. As is commonly done, it was assumed

This document is a research report submitted to the U.S. Department of Justice. This report has not been published by the Department. Opinions or points of view expressed are those of the author(s) and do not necessarily reflect the official position or policies of the U.S. Department of Justice.

that the x values were measured without error. In this model, the a and b values correspond to the initial and final fluorescence values, respectively, while the c value follows the changes in C_t. The d value in the model describes the efficiency of the reactions, as it relates to the slope of the curve in the linear phase. The results were plotted in Figure 12 which illustrates the fit to the two main modes of inhibition and their effect on real-time PCR kinetics. Figure 12A illustrates the effect of loss of template due to inhibitor binding to DNA. The slope and shape of the sigmoidal curve remains constant but there is an increase in C_T. Alternatively, Figure12B illustrates the effect of inhibition on *Taq* polymerase. An increase in C_T is also observed, but in this case, the increase is due to inhibitory effects on the *Taq* polymerase. In both situations, as the concentration of inhibitor increases a gradual loss of product also occurs (change in F_{max}). The results of this model show exceptional fits for both modes of inhibition using tannic acid and bile salts as examples. Results are also provided for three inhibitors: tannic acid (*Taq* polymerase inhibitor), bile salts (DNA binding inhibitor), and phenol (mixed mode inhibitor).

A 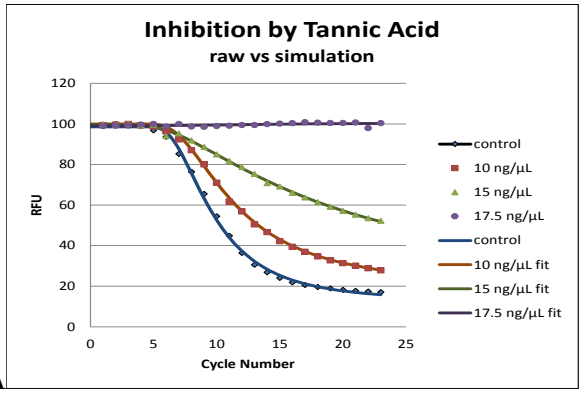

B 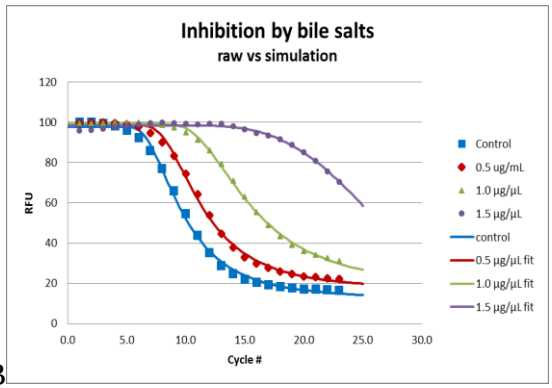

Figure 12. Comparison of two models of PCR inhibition curves using the Weibull Model at the following concentrations of bile salts: 0 µg (red), 0.5 µg/µl (blue), 1 µg/µl (green), 1.5 µg/µl (purple). Raw data and Weibull simulation of the effect of increasing concentration of bile salts, an inhibitor that binds to DNA, 12B: Raw data and Weibull simulation of the effects of increasing concentrations of Tannic acid, a *Taq* polymerase inhibitor. The fits were produced using CurveExpert software based on the raw data created by adding increasing concentrations of each inhibitor to the Plexor® HY real-time PCR Quantification kit. Values for each curve are listed in Table 3.

This document is a research report submitted to the U.S. Department of Justice. This report has not been published by the Department. Opinions or points of view expressed are those of the author(s) and do not necessarily reflect the official position or policies of the U.S. Department of Justice.

Examination of data for three different types of inhibitors in Table 3 shows that for tannic acid, the d term which is related to the exponential slope decreases, while it is quite stable in the bile salt example where the slope varies little until the concentration of the inhibitor reaches 30 µg/µL. The c term also decreases in this example. Conversely in the bile salt sample the c term increases, while the d term remains stable until inhibition reaches the highest levels. Phenol, a mixed mode inhibitor, produces a response much like tannic acid, as would be expected as this data reflects only the slope effects and does not reflect melt curve differences.

Table 3: A list of Weibull fit parameters determined for a set of Plexor® HY real-time autosomal amplification curves. The data show the effect of increased concentration of three PCR inhibitors (tannic acid, bile salts, and phenol) on the reaction curves.

Tannic acid	**a**	**b**	**c**	**d**
Control 0 ng/µL	99	86	1408	-3.35
10 ng/µL	99	82	1617	-3.37
15 ng/µL	99	83	807	-3.00
17.5 ng/µL	99	80	494	-2.68
20 ng/µL	100	82	249	-2.28
22.5 ng/µL	100	87	35.5	-1.30
Bile Salts	**a**	**b**	**c**	**d**
Control 0 µg/ µL	98	86	2333	-3.57
0.5 µg/µL	99	82	7641	-3.82
1 µg/µL	99	81	20208	-3.74
1.5 µg/µL	99	48	435	-1.60
Phenol	**a**	**b**	**c**	**d**
Control 0 µg/µL	99	87	2896	-3.61
33 µg/µL	98	86	1760	-3.33
66 µg/µL	99	84	2807	-3.50
83 µg/µL	99	82	993	-2.87
100 µg/µL	99	80	699	-2.60

This document is a research report submitted to the U.S. Department of Justice. This report has not been published by the Department. Opinions or points of view expressed are those of the author(s) and do not necessarily reflect the official position or policies of the U.S. Department of Justice.

STR summary

The results for PowerPlex® 16 HS, shown in Figures 13-15 and Table 3 demonstrate the effect of PCR inhibition for a subset of the samples described above. STR results inhibited by calcium showed a generic loss of larger alleles (Figure 13). This effect is commonly seen in all inhibitors because smaller loci have more resistance to inhibition (12).

For humic acid (Figure 14) and other inhibitors that bind to DNA, a different pattern of inhibition, allele drop-out, and decreased peak intensity was seen. Sequence-specific and size-dependent reductions in peak intensity occur showing loss of the same loci found with calcium as well as decreased peak intensity in the smaller loci and drop-out in the penta D locus.

Collagen STR results (Figure 15) showed effects on the polymerase and locus-specific inhibitor binding to DNA. Due to the improved inhibition resistance of the STR kit, higher concentrations of collagen were used when compared to the real time results. With respect to the effects of inhibition on STR amplification, (Table 2), collagen affected a greater number of loci. Interestingly, phenol and EDTA produced drop-out and decreased peak intensity of the same loci as collagen. Urea produced allele drop-out and decreased peak intensity of two additional loci. These results are consistent with a mixed mode effect - inhibitor binding both *Taq* polymerase and DNA.

This document is a research report submitted to the U.S. Department of Justice. This report has not been published by the Department. Opinions or points of view expressed are those of the author(s) and do not necessarily reflect the official position or policies of the U.S. Department of Justice.

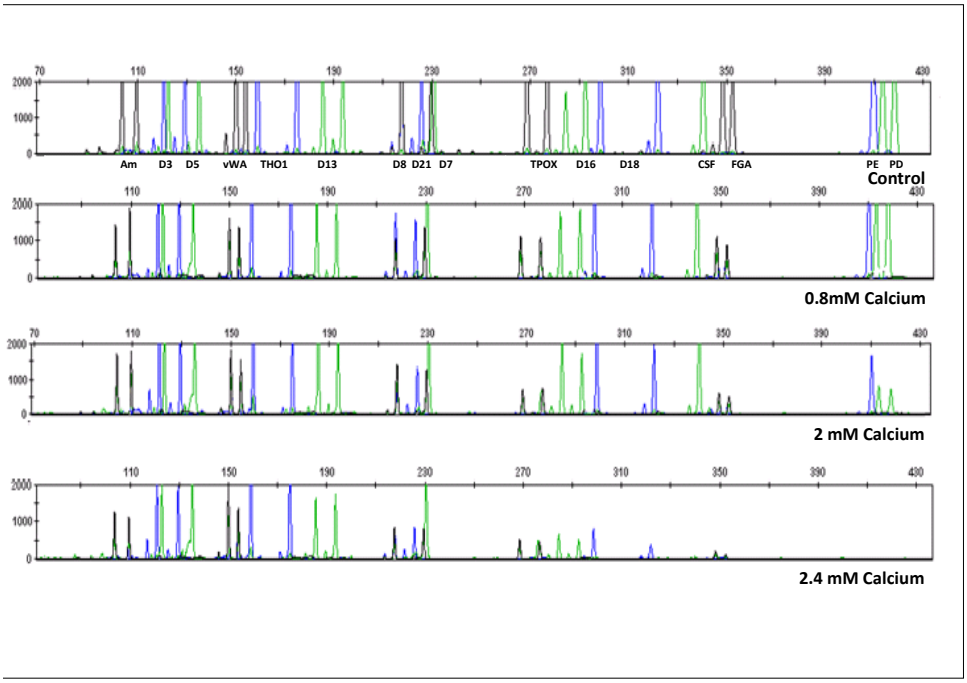

Figure 13: PowerPlex® 16 HS amplification results with increasing concentrations of calcium. Allele drop-out observed at 2.4 mM final concentration for 0.5 ng input DNA.

This document is a research report submitted to the U.S. Department of Justice. This report has not been published by the Department. Opinions or points of view expressed are those of the author(s) and do not necessarily reflect the official position or policies of the U.S. Department of Justice.

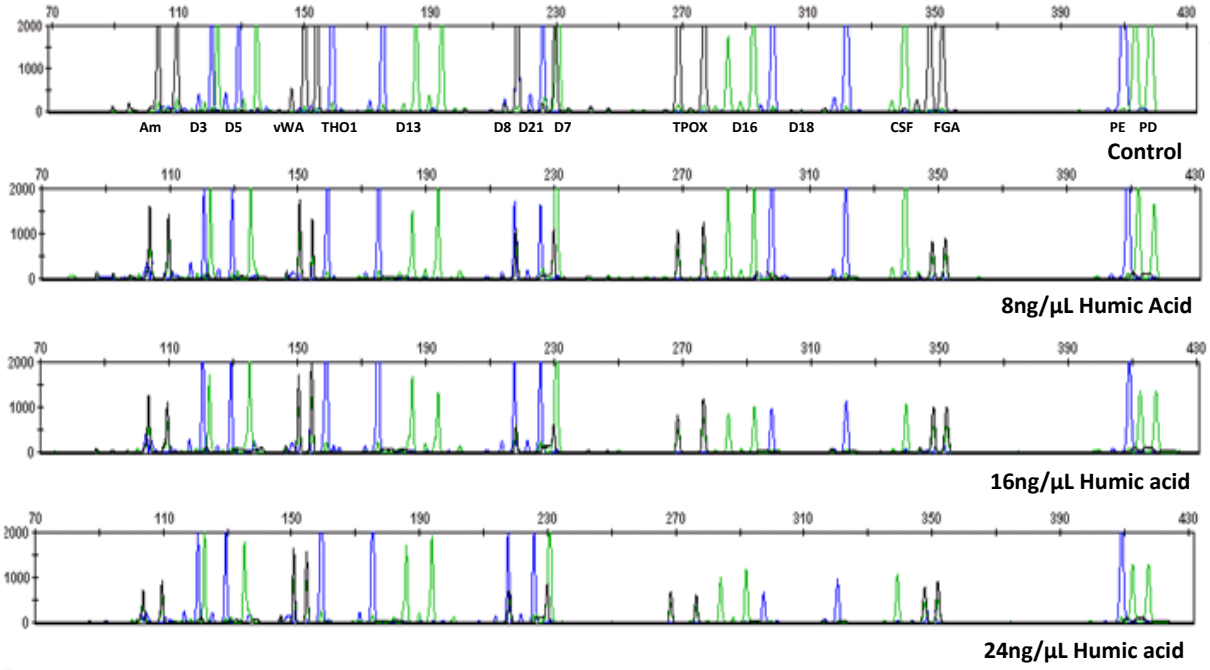

Figure 14: PowerPlex® 16 HS amplification results with increasing concentrations of Humic Acid, PCR inhibition increases with concentration of humic acid, 0.5 ng input DNA.

This document is a research report submitted to the U.S. Department of Justice. This report has not been published by the Department. Opinions or points of view expressed are those of the author(s) and do not necessarily reflect the official position or policies of the U.S. Department of Justice.

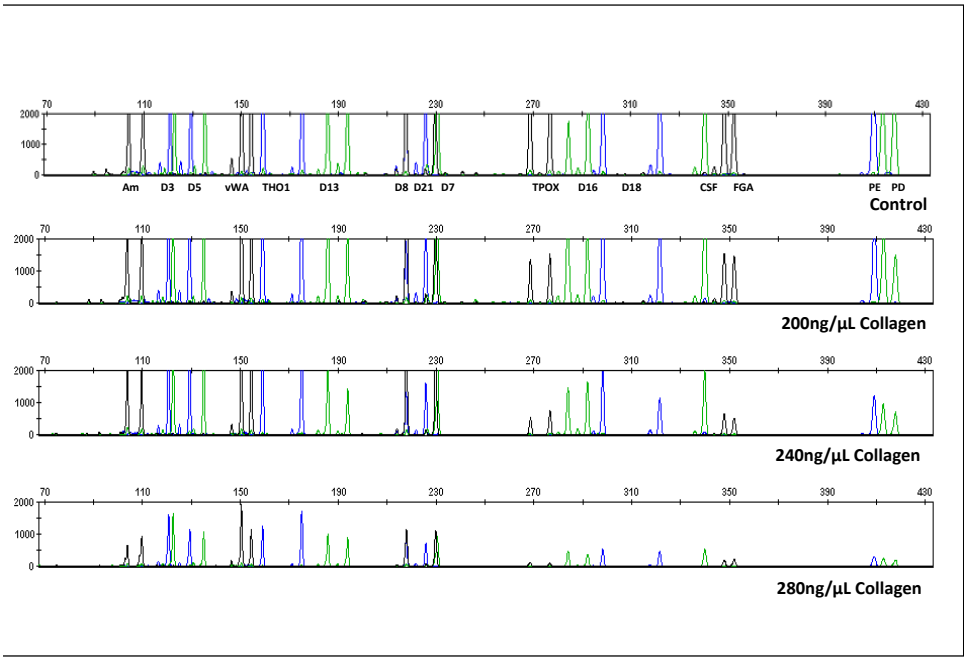

Figure 15: PowerPlex® 16 HS amplification results with increasing concentrations of collagen. Allele drop-out observed at 280 ng/µL for 0.5 ng input DNA.

Discussion

In analysis of inhibition by qPCR, several mechanisms have been observed using a variety of known PCR inhibitors that affect the reaction in three modes of action. Inhibitors such as calcium and tannic acid seem to interfere with the *Taq* polymerase potentially through binding or interfering with the magnesium cofactor. For those inhibitors that may bind to the DNA by intercalating or groove binding, such as humic acid, the sequence of the amplicon as well as molecular structure are likely to determine the level of inhibition. Melanin and bile salts possibly interfere with the DNA molecule through the formation of complexes. The remaining inhibitors experienced a mixed mode effect by interfering with both the DNA and *Taq* polymerase. Although these inhibitors show similar modes of inhibiton, their inhibition techniques may vary.

This document is a research report submitted to the U.S. Department of Justice. This report has not been published by the Department. Opinions or points of view expressed are those of the author(s) and do not necessarily reflect the official position or policies of the U.S. Department of Justice.

Urea and guanidinium, for example, are similar in structure and bind to both DNA and *Taq* polymerase; however, one facilitates denaturation and the other promotes hydrogen bonding of the complementary basepairs, keeping the dsDNA intact.

In commercial kits for qPCR assays, addition of BSA to the reaction mix reduces inhibition and is one of the few treatments that does not dilute the sample. Other treatments, including purification with silica-based spin columns or rinsing the sample with NaOH result in a loss of DNA template (17,48). Purification of the sample with low melting temperature agarose can remove inhibitors but the DNA template is diluted by half (18). Therefore, for samples that are highly degraded or of low template DNA, these methods are not feasible. Knowledge of the type of inhibitor present, based on the qPCR data, will help analysts select the method which would effectively remove the inhibitors without compromising the amount of DNA or further compromising the PCR reaction. Future research in this area could begin to classify inhibitors based on specific treatment methods.

The application of qPCR to detect inhibition can provide useful data for laboratories confronted with such samples. Inhibitors such as calcium, humic acid and collagen affect STR amplification in different ways (12,16). Depending on the type of inhibition, different effects can be seen in the STR results (16). Sequence-specific inhibition and allele drop-out is often seen with inhibitors that bind DNA. However, allele drop-out does not necessarily mean inhibition, as degraded and low template samples can produce similar results. Detection of inhibition using STR results may not always be possible, which is why qPCR data and melt curve analysis can be so useful when poor results are seen. The results presented in this paper demonstrate that melt curve analysis combined with qPCR can aid in the prediction of PCR inhibition. In the future, the effects of inhibition will continue to need to be assessed through qPCR assays and STR analysis. This information will positively impact the forensic community by giving more complete information on the various types of inhibitors and their modes of action.

This document is a research report submitted to the U.S. Department of Justice. This report has not been published by the Department. Opinions or points of view expressed are those of the author(s) and do not necessarily reflect the official position or policies of the U.S. Department of Justice.

Acknowledgments

The authors would like to thank Promega Corporation for their technical support of this project and Kerry Opel, Derrick Duncan, Arianna Pionzio, Garrett English, and Steve Winkle for their insightful comments and suggestions in this research area. This project was supported through NIJ grant # 2010-DN-BX-K204. Points of view in the document are those of the authors and do not necessarily represent the official view of the US Department of Justice.

References

1. Bessetti J. An introduction to PCR inhibitors. Profiles in DNA 2007; 10(1) 9-10.

2. Wilson I. Inhibition and facilitation of nucleic acid amplification. Appl. Environ. Microbiol. 1997;63(10):3741-51.

3. Hartzell B, McCord B. Effect of divalent metal ions on DNA studied by capillary electrophoresis. Electrophoresis 2005;26:1046-56.

4. Demeke T, Jenkins GR. Influence of DNA extraction methods, PCR inhibitors and quantification methods on real-time PCR assay of biotechnology-derived traits. Anal. Bioanal. Chem. 2010;396:1977–90.

5. Butler JM. Forensic DNA typing, second edition: biology, technology, and genetics of STR markers; Elsevier Academic Press: London, UK, 2005.

6. Higuchi R, Fockler C, Dollinger G, Watson R. Kinetic PCR: Real-time monitoring of DNA amplification reactions. Biotechnology 1993;11:1026–30.

7. Heid CA, Stevens J, Livak KJ, Williams PM. Real-time quantitative PCR. Genome 1998;6:986-94.

8. Holland PM, Abramson RD, Watson R, Gelfand DH. Detection of specific polymerase chain reaction product by utilizing the 5'----3' exonuclease activity of *Thermus aquaticus* DNA polymerase. Proc. Nat. Acad. Sci. USA 1991;88(16):7276–80.

9. Krenke B, Nassif N, Sprecher C, Knox S, Schwandt M, Storts DR. Developmental validation of a real-time PCR assay for the simultaneous quantification of total human and male DNA. For. Sci. Int. Genet.

This document is a research report submitted to the U.S. Department of Justice. This report has not been published by the Department. Opinions or points of view expressed are those of the author(s) and do not necessarily reflect the official position or policies of the U.S. Department of Justice.

2008;3:14-28.

10. Johnson SC, Sherrill CB, Marshall DJ, Moser MJ, Prudent JR. A third basepair for the polymerase chain reaction: Inserting isoC and isoG. Nucleic Acids Res. 2004;32(6):1937-41.

11. Ririe KM, Rasmussen RP, Wittwer CT. Product differentiation by analysis of DNA melting curves during the polymerase chain reaction. Anal Biochem. 1997;245(2):154- 60.

12. Opel K, Chung D, McCord BR. A study of PCR inhibition mechanisms using real-time PCR. J. Forensic Sci. 2010;55(1):25-33.

13. Kolk AHJ, Noordhoek GT, De Leeuw O, Kuijper S, and Van Embden JDA. *Mycobacterium smegmatis* strain for detection of *Mycobacterium tuberculosis* by PCR used as internal control for inhibition of amplification and for quantitation of bacteria. J. Clin. Microbiol. 1994;32:1354-6.

14. Guescini M, Sisti D, Rocchi M., Stocchi L, Stocchi V. A new real-time PCR method to overcome significant quantitative inaccuracy due to slight amplification inhibition, BMC Bioinformatics 2008;9:326:1-12

15. Richards FJ: A flexible growth function for empirical use. Journal of Experimental Botany 1959; 10:290-300.

16. Funes-Huacca ME, Opel K, Thompson R, McCord BR. A comparison of the effects of PCR inhibition in quantitative PCR and forensic STR analysis. Electrophoresis 2011;32(9):1084-9.

17. Bourke MT, Scherczinger CA, Ladd C, Lee HC. NaOH treatment to neutralize inhibitors of *Taq* polymerase. J. Forensic Sci. 1999;44(5):1046-50.

18. Alaeddini, R. Forensic implications of PCR inhibition – A review, Forensic Sci. Int Genetics 2011;6:297-305.

19. Ensengerger MG, Thompson J, Hill B, Homick K, Kearney V, Mayntz-Press KA, et al. Developmental validation of the Poweplex® 16 HS System: an improved 16-locus fluorescent STR multiplex. Forensic Sci Int Genet. 2010 4(4):257-64.

This document is a research report submitted to the U.S. Department of Justice. This report has not been published by the Department. Opinions or points of view expressed are those of the author(s) and do not necessarily reflect the official position or policies of the U.S. Department of Justice.

20. Mulero J, Chang C, Lagacé RE, Wang D, Bas JL, McMahon T, Hennessy L, Development and validation of the **AmpFℓSTR® MiniFiler™** PCR amplification kit: a MiniSTR multiplex for the analysis of degraded and/or PCR inhibited DNA. J. Forensic Sci., 53 (4):838-52.

21. Comey CT, Koons BW, Presley KW, Smerick JB, Sobieralski CA, Stanley DM. DNA extraction strategies for amplified fragment length polymorphisms. J Forensic Sci. 1994;39(5):1254–69.

22. Promega Corporation. Plexor ®HY system for the Corbett Rotor-gene 6000 series detection system technical manual. 2009.

23. Ruijter JM, van der Velden S, Ilgun A. LinRegPCR: Analysis of quantitative RT-PCR data [computer program]. Version 11.0. Heart Failure Research Center, Academic Medical Centre: Amsterdam, The Netherlands: 2009.

24. Kontanis EJ, Reed FA. Evaluation of real-time PCR amplification efficiencies to detect PCR inhibitors. J. Forensic Sci. 2006;51(4):795-804.

25. Promega Corporation. Poweplexr® ®16 HS system technical manual. 2009.

26. Bickley J, Short JK, McDowell G, Parkes HC. Polymerase chain reaction (PCR) detection of *Listeria monocytogenes* in diluted milk and reversal of PCR inhibition caused by calcium ions. Lett. Appl. Microbiol. 2008;22(2):153-8.

27. Zipper H, Buta C, Lämmle K, Brunner H, Bernhagen J, Vitzthum F. Mechanisms underlying the impact of humic acids on DNA quantification by SYBR Green I and consequences for the analysis of soils and aquatic sediments. Nucleic Acids Res. 2003;31(7):e39

28. Sutlovic D, Gamulin S, Definis-Gojanovic M, Gugic D, Andjelinovic S. Interaction of humic acids with human DNA: proposed mechanisms and kinetics. Electrophoresis 2008; 29(7):1467-72.

29. Tebbe CC, Vahjen W. Interference of humic acids and DNA extracted directly from soil in detection and transformation of recombinant DNA from bacteria and a yeast. Appl. Environ. Microbiol. 1993;59(8):2657-65.

30. Scholz M, Giddings I, Pusch CM. A polymerase chain reaction inhibitor of ancient hard and soft

This document is a research report submitted to the U.S. Department of Justice. This report has not been published by the Department. Opinions or points of view expressed are those of the author(s) and do not necessarily reflect the official position or policies of the U.S. Department of Justice.

tissue DNA extracts is determined as human collagen type I. Anal. Biochem. 1998;259(2):283-6.

31. Mrevlishvili GM, Svintradze DV. Complex between triple helix of collagen and double helix of DNA in aqueous solution. Int. J. Biol. Macromol. 2005;35(5):243-5.

32. Pidaparti RM, Svintradze DV, Shan Y, Yokota H. Optimization of hydrogen bonds for combined DNA/collagen complex. J. Theor. Biol. 2009;256(2):149-56.

33. Goldar A, Sikorav JL. DNA renaturation at the water-phenol interface. Eur. Phys. J. E. 2004; 14:211–39.

34. Katcher HL, Schwartz I. A distinctive property of *Tth* DNA polymerase: enzymatic amplification in the presence of phenol. BioTechniques 1994;16:84-92.

35. Wiedbrauk DL, Werner JC, Drevon AM. Inhibition of PCR by aqueous and vitreous fluids. J. Clin. Microbiol. 1995;33(10):2643-6.

36. Akane A, Matsubara K, Nakamura H, Takahashi S, Kimura K. Identification of the heme compound copurified with deoxyribonucleic acid (DNA) from bloodstains, a major inhibitor of polymerase chain reaction (PCR) amplification. J. Forensic Sci. 1994; 39:362-72.

37. Yoshii T, Tamura K, Taniguchi T, Akiyama K, Ishiyama I. Water-soluble eumelanin as a PCR-inhibitor and a simple method for its removal. Nippon Hoigaku Zasshi 1993; 47(323):329.

38. Geng J, Yuan P, Shao C, Yu S, Zhou B, Zhou P, Chen X. Bacterial melanin interacts with double-stranded DNA with high affinity and may inhibit cell metabolism in vivo. Arch. Microbiol. 2010;192:321-9.

39. Eckhart L, Bach J, Ban J, Tschachler E. Melanin binds reversibly to thermostable DNA polymerase and inhibits its activity. Biochem. Biophys. Res. Commun. 2000;271: 726-730.

40. Kreader CA. Relief of amplification inhibition in PCR with bovine serum albumin or T4 gene 32 protein. Appl. Environ. Microbiol. 1996;62(3):1102-6.

41. Merritt ME, Donaldson JR. Effect of bile salts on the DNA and membrane integrity of enteric bacteria. J. Med. Microbiol. 2009;58:1533-41.

42. Khan G, Kangro HO, Coates PJ, Heath RB. Inhibitory effects of urine on the polymerase chain

This document is a research report submitted to the U.S. Department of Justice. This report has not been published by the Department. Opinions or points of view expressed are those of the author(s) and do not necessarily reflect the official position or policies of the U.S. Department of Justice.

reaction for Cytomegalovirus DNA. J. Clin. Pathol. 1991;44:360-5

43. Wadsworth JDF, Hill AF, Joiner S, Jackson GS, Clarke AR, Collinge J. Strain-specific prion-protein conformation determined by metal ions. Nat. Cell Biol. 1999;1:55-9.

44. Sundberg MW, Meares CF, Goodwin DA, Diamanti CI. Selective binding of metal ions to macromolecules using bifunctional analogs of EDTA. J. Med. Chem. 1974;17(12):1304-7.

45. Seto, H.; Tomasz, A. Early stages in DNA binding and uptake during genetic transformation of *Pneumococci.* Proc. Nat. Acad. Sci. USA 1977;71(4):1493-8.

46. Makowski GS, Davis EL, Hopfer SM. Amplification of Guthrie card DNA: effects of guanidine thiocyanate on binding of natural whole blood PCR inhibitors. J. Clin. Lab. Anal. 1997;11:87-93.

47. García-Pérez M, Pinto M, Subirana JA. Nonsequence-specific arginine interactions in the nucleosome core particle. Biopolymers 2003;69(4):432-439.

48. Yang D, Eng B, Waye JS, Dudar JC, Saunders SR. Improved DNA extraction from ancient bones using silica based spin columns. Am J Phys Anthropol 1998;105:539-43.

49. Phillipe, J.R ZunZun.com, Online curve fitting and surface fitting web site, accessed 8/26/2012.

50. Hyams, DG., "CurveExpert Professional" software, http://www.curveexpert.net

accessed 8/26/12.

51. Tjørve, E. Shapes and functions of species–area curves: a review of possible models J. Biogeogr. 2003;30:827–35.

52. Weibull, W. A statistical distribution function of wide applicability. J. Appl. Mech.1951;18:293–6.

53. Yang RC., Kozak, A, Smith JHG. The potential of Weibull-type functions as flexible growth curves. Can. J. Forest Res. 1978;8:424–31.

54. Reid, D. The effects of frequency of defoliation on the yield response of a perennial ryegrass sward to a wide range of nitrogen application rates. J. Agr. Sci. 1978;90:447–57.

55. Revzin, A. Techniques for characterizing nonspecific protein DNA interactions In: Revzin

This document is a research report submitted to the U.S. Department of Justice. This report has not been published by the Department. Opinions or points of view expressed are those of the author(s) and do not necessarily reflect the official position or policies of the U.S. Department of Justice.

Part II. The Effect of Internal Control Sequence and Length on the Response to PCR Inhibition in Real-Time PCR Quantitation

Introduction

A key step in producing a DNA profile is to determine the concentration of DNA present in an extracted sample. Once this is known an optimal volume of sample can then be added to the subsequent STR amplification. This is commonly performed by real time PCR, which can be a sensitive and human specific DNA-quantification technique when used with appropriate primer sets. However, DNA samples of forensic interest do not always come from the most pristine conditions and often contain co-extractable PCR inhibitors. These inhibitors can be detected in a DNA sample using real time PCR by including a non-human target in each reaction tube, and examining the respective cycle threshold (C_t) values for this amplicon [1]. The internal control sequence is added at a set concentration, and should therefore produce a constant C_t value for each reaction. However, if an inhibitory substance is present in a particular sample, the normally constant C_t value for the internal control sequence may be increased as the inhibitor can block access to the DNA template. In addition, co-extracted inhibitors can alter amplification efficiency and affect the melt temperature (T_m) of the amplified DNA [2, 3, 4]. Increases in the C_t value of the real time PCR amplification internal control generally indicate the presence of interfering substances which affect the ability of the polymerase to amplify the DNA. It is expected that such inhibitors would affect the unknown quantity of DNA template and the known amount of internal control DNA in a similar fashion. This increase in C_t is likely the result of the inhibitor binding to the DNA or sterically hindering it, thereby reducing the total amount of accessable DNA template [1]. When such a process occurs, it is reasonable to expect changes in the melt curves due to increasing interactions with the double stranded DNA. Of course it is also possible for the inhibitor to affect the *Taq* polymerase by partially disabling it resulting in a reduction in the processivity of the enzyme. Inhibitors that alter *Taq* processivity tend to produce changes in amplification efficiency, altering the shape and slope of the real

This document is a research report submitted to the U.S. Department of Justice. This report has not been published by the Department. Opinions or points of view expressed are those of the author(s) and do not necessarily reflect the official position or policies of the U.S. Department of Justice.

time amplification curve. For example, inhibitors such as $Ca^{++,}$ may prevent the Mg^{++} ions from interacting with the enzyme, which results in sub-optimal performance or deactivation of the *Taq*, [1].

Ultimately, PCR inhibition is manifested by a reduction in intensity or a complete loss of alleles following the multiplex PCR amplification of STRs. The inhibition can be generic, resulting in the loss of larger alleles; or it can be more specific, affecting certain alleles more than others, regardless of size. One method of alleviating these inhibitory effects is by diluting the DNA sample [5]; however, dilution decreases the concentration of the DNA as well as the inhibitor. Better understanding of the mechanism of inhibition would permit the user to develop specific mitigation techniques such as spin filtration, the addition of BSA, or the use of smaller amplicons, based upon the real time response [6]. Another challenge is the choice of internal control length and sequence. A variety of real time PCR kits exist, each with different control sequence lengths and chemistries. Anecdotal evidence suggests that the internal control sequences in these kits vary in response to different inhibitors.

Thus, in this study we examine the effects of commonly encountered PCR inhibitors on internal controls of varying amplicon length and sequence structure, hypothesizing that the sequences with greater guanine and cytosine content and smaller length would be the least prone to inhibitory interactions as they are more thermodynamically stable and less capable of binding larger inhibtiors. Using the data generated from this study, it should be possible to improve the response of real time PCR methods by developing more responsive IPC probes, and improving the ability of laboratories to understand and detect PCR inhibition.

Materials and Methods

IPC DNA and primer sequences

Three 400bp DNA sequences were randomly generated to create IPCs with 53%, 44% and 32% GC content based upon the range seen in typical forensic STRs. The sequences were run against the nucleotide BLAST database [7], and only those with no match to any known sequences were chosen. These were ordered from Integrated DNA Technologies (IDT) as a custom gene sequence [8]. Forward

This document is a research report submitted to the U.S. Department of Justice. This report has not been published by the Department. Opinions or points of view expressed are those of the author(s) and do not necessarily reflect the official position or policies of the U.S. Department of Justice.

and reverse primers were designed using Primer3 [9] and unlabeled primers were synthesized by IDT [9]. The reverse primer targets were placed within the main sequence to create a total amplicon length of 80bp, 160bp and 230bp. The forward IPC primer was labeled at the 5'-end with an Iso-C base and Cal-Fluo-Red 610 fluorescent tag (BioSearch Technologies [10]) for use with the Plexor® HY System (Promega Corporation, Madison, WI).

Inhibitors

Inhibitor stocks of tannic acid, bile salts, collagen, guanidinium isothyanate, hematin, humic acid, melanin and urea were made according to Opel et al. [1] and subsequent dilutions were made with water. In previous research [13], we found tannic acid to be a *Taq* polymerase inhibitor, while bile salts, humic acid, hematin, and melanin were DNA binding inhibitors. Lastly guanidinium, urea and collagen acted as mixed mode inhibitors, affecting both the polymerase and the DNA template [13]. Thus these inhibitors provided a wide range of differing effects to test our hypothesis.

PCR reactions

Volumes of master mix, primer mix and DNA were prepared per reaction according to manufacturer's specifications [11], where up to 5µL of the 7µL of water was replaced with inhibitor to get the final concentrations listed in Table 1. Each of the nine individual IPC amplicon sequences was performed in triplicate at each inhibitor concentration and the average change in C_t, efficiency and T_m was determined for the uninhibited control and for the concentration where 50% inhibition occurred. The sequences that produced the greatest change in each of the 3 criteria were tallied to identify which amplicon was the most impacted by inhibition.

Sample analysis

Cycle threshold values and melt temperatures were obtained using the Plexor Analysis Software version 1.5.4.18 [12]. The real time amplification curves were simulated using the Weibull Model, as by

This document is a research report submitted to the U.S. Department of Justice. This report has not been published by the Department. Opinions or points of view expressed are those of the author(s) and do not necessarily reflect the official position or policies of the U.S. Department of Justice.

Thompson [13] and the reaction efficiencies were estimated using the slope value of the Weibull function given as $y = a - b^{(-cx^{\wedge}d)}$ in CurveExpert Professional version 1.6.0 [14]. This sigmoidal regression uses all of the points in the amplification to generate an equation to the PCR amplification curve. The Weibull d variable can be used as an estimate of the linear slope of the amplification the curve; this value can then be used to estimate reaction efficiency when R^2 values are 0.99 or greater [15]. Control PCR amplifications with no inhibitor present were assumed to amplify with the greatest efficiency, and all subsequent inhibited amplification efficiencies are represented as a percentage thereof.

Pairwise comparisons were performed on the average values of the control to the average values of the second inhibitor concentration (Table 1) for each amplicon of each inhibitor to determine the significance of changes seen in cycle threshold, melt temperature and efficiency values using IBM SPSS Statistics for Windows, Version 20.0 (IBM Corporation, Armonk, NY).

Inhibitor	Type	Sources	Final reaction concentrations
Bile salts	DNA	Feces	0, 0.5, 1.0, 1.5µg/µL
Collagen	Mixed	Bone, tissue	0, 25, 50, 75, 87.5, 100, 112.5ng/µL
Guanidinium	Mixed	Guanidinium salts	0, 1.5, 4.5, 7.5ng/µL
Hematin	DNA	Blood	0, 15, 30, 45, 60, 75, 90µM
Humic acid	DNA	Soils	0, 10, 20, 30, 40, 60ng/µL
Melanin	DNA	Hair, tissue	0, 20, 40, 60ng/µL
Tannic acid	*Taq*	Leather, plant material	0, 7.5, 11.25, 18.5ng/µL
Urea	Mixed	Urine	0, 100, 300, 500mM

Table 1: List of inhibitors, their mode of inhibition and common sources, along with each reaction's final inhibitor concentration.

Results and Discussion

The goal of these experiments was to examine the overall ability of different internal control sequences to predict the presence of PCR inhibition. More specifically, we were interested in the ways variations in concentration of different PCR inhibitors impacted amplicons of different length and sequence. Our overall results indicated that the amplicon size can have more of an influence on the degree of inhibition than the specific amplicon sequence. The sequence can also have an effect if the

This document is a research report submitted to the U.S. Department of Justice. This report has not been published by the Department. Opinions or points of view expressed are those of the author(s) and do not necessarily reflect the official position or policies of the U.S. Department of Justice.

inhibitor interacts more directly with the DNA, rather than with the polymerase. For example, Bile salts produced pronounced inhibition with amplicon sequences containing 53% GC content, where the greatest changes in efficiency, C_t and T_m occurred. Similar effects were seen in other DNA interacting inhibitors, as shown in Tables 2 and 3 and Figure 1. Polymerase inhibitors do not show as pronounced of a difference between sequences as the DNA interacting inhibitors, however IPCs with 32% GC content did show more inhibition than the other sequences for certain mixed modal inhibitors, such as collagen (Table 4).

Δ C_t	Bile salts	Collagen	Guanidinium	Hematin	Humic Acid	Melanin	Tannic Acid	Urea
	1.0ng/µL	100ng/µL	4.5ng/µL	60uM	40ng/µL	16ng/µL	11.25ng/µL	300mM
Autosomal	1.63±0.03	**3.8±0.2**	0.2±0.03	**2.0±0.2**	**2.5±0.2**	**2.3±0.22**	**0.6±0.06**	**1.9±0.15**
Y	**1.4±0.1**	**5.2±0.1**	**1.9±0.12**	**4.3±0.1**	**2.4±0.2**	**1.4±0.1**	**1.3±0.1**	**1.4±0.3**
53% GC 80bp	**1.1±0.1**	**2.3±0.03**	0.1±0.03	**1.6±0.07**	**1.07±0.07**	**1.4±0.06**	-0.3±0.0	**0.9±0.06**
53% GC 160bp	**2.6±0.1**	***9.8±0.8***	**1.3±0.0**	**0.4±0.03**	**1.3±0.0**	**1.3±0.07**	**1.3±0.07**	**1.0±0.03**
53% GC 230bp	***14.8±0.9***	**8.6±1.2**	**0.6±0.0**	**2.3±0.2**	**1.7±0.09**	**3.07±0.03**	**2.1±0.03**	**2.1±0.06**
44% GC 80bp	**1.5±0.07**	**1.8±0.0**	**-0.3±0.0**	**1.3±0.03**	**2.3±0.4**	**2.0±0.03**	**1.7±0.03**	**1.2±0.03**
44% GC 160bp	**3.9±0.03**	**4.9±0.0**	**1.1±0.0**	**1.7±0.03**	**1.7±0.0**	**1.2±0.0**	**0.5±0.06**	**2.7±0.0**
44% GC 230bp	**4.7±0.5**	**5.35±0.2**	***2.5±0.03***	**2.9±0.23**	**1.1±0.03**	***4.1±0.3***	**2.2±0.0**	**2.7±0.03**
32% GC 80bp	**0.9±0.03**	**1.6±0.07**	**-0.6±0.03**	**1.7±0.03**	**1.9±0.1**	**2.7±0.07**	**0.3±0.1**	**1.0±0.03**
32% GC 160bp	**2.1±0.03**	**5.9±0.03**	0.0±0.0	**2.9±0.1**	**2.7±0.03**	**1.7±0.0**	***2.5±0.03***	**2.07±0.03**
32% GC 230bp	**11.2±0.9**	**5.9±0.1**	**2.0±0.03**	***3.7±0.1***	***4.07±0.03***	**2.8±0.03**	**1.8±0.03**	***4.07±0.03***

Table 2: The average change in C_t from the control to the described inhibited sample ± the standard error. All boldface samples indicate a significant change from the control where $p<0.05$. Highlighted and italicized samples indicate the amplicon most affected by the presence of the inhibitor.

This document is a research report submitted to the U.S. Department of Justice. This report has not been published by the Department. Opinions or points of view expressed are those of the author(s) and do not necessarily reflect the official position or policies of the U.S. Department of Justice.

Δ Melt	Bile salts	Collagen	Guanidinium	Hematin	Humic Acid	Melanin	Tannic Acid	Urea
	1.0ng/µL	100ng/µL	4.5ng/µL	60uM	40ng/µL	16ng/µL	11.25ng/µL	300mM
Autosomal	**-0.5±0.0**	**2.4±0.0**	**2.2±0.0**	-0.2±0.0	2.5±0.2	-0.4±0.0	-0.1±0.0	**-0.9±0.0**
Y	**-0.6±0.0**	**2.0±0.0**	**2.4±0.0**	0.0±0.0	2.4±0.2	-0.2±0.0	-0.03±0.03	**-0.7±0.0**
53% GC 80bp	**-0.4±0.0**	**1.8±0.03**	**2.6±0.06**	0.0±0.03	1.1±0.1	***-0.3±0.0***	0.0±0.04	**-0.7±0.03**
53% GC 160bp	***-0.6±0.0***	**2.0±0.03**	**2.4±0.0**	0.03±0.03	1.3±0.0	-0.2±0.03	0.07±0.03	**-0.5±0.0**
53% GC 230bp	**-0.3±0.0**	**2.0±0.03**	**2.5±0.0**	0.03±0.03	1.7±0.09	-0.1±0.03	0.0±0.0	**-0.4±0.03**
44% GC 80bp	**-0.3±0.0**	**2.0±0.03**	**2.7±0.0**	0.0±0.0	2.3±0.4	-0.1±0.03	0.03±0.03	**-0.7±0.0**
44% GC 160bp	**-0.5±0.03**	**2.0±0.03**	**2.8±0.03**	0.03±0.03	1.7±0.0	-0.03±0.03	0.03±0.0	**-0.6±0.0**
44% GC 230bp	**-0.5±0.0**	***2.1±0.03***	**2.9±0.03**	0.07±0.03	1.1±0.0	**0.1±0.0**	0.1±0.03	**-0.2±0.03**
32% GC 80bp	**-0.3±0.0**	**1.9±0.0**	**2.7±0.03**	-0.07±0.03	1.9±0.1	**-0.2±0.0**	-0.1±0.0	***-0.9±0.03***
32% GC 160bp	**-0.4±0.0**	***2.1±0.03***	**2.8±0.03**	0.03±0.0	2.7±0.0	-0.03±0.03	0.07±0.03	**-0.7±0.03**
32% GC 230bp	**-0.2±0.0**	**2.1±0.03**	***2.9±0.0***	0.1±0.0	4.1±0.0	**-0.1±0.0**	-0.07±0.03	**-0.5±0.0**

Table 3: The average change in melt temperature ± the observed standard error from the control to the indicated inhibited concentration. All boldface samples indicate a significant difference between this level of inhibition and the control sample where $p<0.05$. Highlighted and italicized samples indicate the amplicon most affected by the presence of the inhibitor.

% Efficiency	Bile salts	Collagen	Guanidinium	Hematin	Humic Acid	Melanin	Tannic Acid	Urea
	1.0ng/µL	100ng/µL	4.5ng/µL	60uM	40ng/µL	16ng/µL	11.25ng/µL	300mM
Autosomal	**92.4±1.2%**	**87.7±1.0%**	**85.4±0.3%**	**63.5±1.7%**	**57.6±1.9%**	**62.6±2.4%**	**67.8±1.9%**	**53.3±1.7%**
Y	80.9±2.8%	**41.5±4.6%**	**42.0±3.0%**	**10.1±1.9%**	**21.1±2.4%**	**39.6±1.8%**	**33.0±0.2%**	**47.9±4.6%**
53% GC 80bp	93.1±1.8%	**82.9±0.3%**	**71.7±1.5%**	**67.8±2.9%**	**62.2±1.6%**	**72.5±1.9%**	**63.6±5.4%**	**66.1±1.1%**
53% GC 160bp	**69.2±0.6%**	**23.3±2.4%**	**61.1±1.5%**	**70.3±1.3%**	**61.5±8.9%**	**66.2±1.8%**	**61.0±3.2%**	**71.3±0.9%**

This document is a research report submitted to the U.S. Department of Justice. This report has not been published by the Department. Opinions or points of view expressed are those of the author(s) and do not necessarily reflect the official position or policies of the U.S. Department of Justice.

53% GC 230bp	**10.9±1.8%**	**14.0±3.8%**	**61.9±4.0%**	**51.1±0.8%**	**58.3±3.6%**	**54.6±2.1%**	**52.8±0.2%**	**65.6±2.4%**
44% GC 80bp	**88.0±0.2%**	**84.0±1.6%**	**75.1±1.0%**	**64.7±0.8%**	***51.3±3.3%***	**66.9±1.6%**	**75.5±3.9%**	**71.7±1.7%**
44% GC 160bp	**48.1±1.9%**	**48.9±3.8%**	**59.5±1.6%**	**59.5±2.8%**	**53.9±4.2%**	**66.0±0.8%**	**60.9±0.8%**	**68.2±2.4%**
44% GC 230bp	**12.9±3.3%**	***10.3±3.9%***	**63.6±0.9%**	**45.2±4.6%**	**64.9±2.3%**	***42.1±3.6%***	***50.4±1.3%***	**60.0±5.0%**
32% GC 80bp	**90.3±0.3%**	**80.2±1.9%**	**75.6±1.1%**	**55.4±0.6%**	**63.4±0.9%**	**54.7±1.9%**	**67.5±3.0%**	**60.8±3.0%**
32% GC 160bp	**75.1±0.8%**	**52.3±4.2%**	**70.7±1.1%**	**55.0±3.4%**	**58.3±1.6%**	**59.9±1.5%**	**51.8±3.9%**	**60.2±3.0%**
32% GC 230bp	***8.1±0.4%***	**34.8±2.1%**	***49.7±1.8%***	***47.0±2.5%***	**52.0±6.9%**	**54.3±3.6%**	**52.2±2.3%**	***51.4±3.2%***

Table 4: The percentage ± the observed standard error of the efficiency in the inhibited sample relative to the control sequence. All samples significantly decreased in efficiency with the addition of any PCR inhibitor, where $p<0.05$. Highlighted and italicized samples indicate the amplicon most affected by the presence of the inhibitor. In all cases, the control sequence was assumed to be 100% efficient.

Amplicon size

Amplicon size strongly impacts the degree of inhibition for all modes of inhibition in the real-time PCR amplification curves. The changes in efficiency between the 80bp amplicon and the 230bp for any sequence composition show dramatic differences; the largest amplicon fails in many inhibitory concentrations where the smallest amplicon amplifies rather well (Figure 2, Table 4). This is presumably because the larger sequences require a longer interaction with the polymerase and provide a wider range of DNA sequence variations to bind to. This is an expected finding, as inhibitory events commonly cause larger STR loci to drop out first. Unlike Mulero *et al*., we find that when comparing across a range of amplicon sizes, that the short amplicon sizes are more capable of amplifying in the presence of an inhibitor. Previous studies on STR dropout due to inhibition have indicated that the size of the STR can have a greater influence on allele drop out and peak imbalance than the %GC content of the STR [4]. However, as seen in these results, the pattern of inhibitory progression is not identical for all DNA or *Taq* inhibitors as sequence increases in length or GC content. Therefore, it becomes important to examine individual inhibitory effects.

This document is a research report submitted to the U.S. Department of Justice. This report has not been published by the Department. Opinions or points of view expressed are those of the author(s) and do not necessarily reflect the official position or policies of the U.S. Department of Justice.

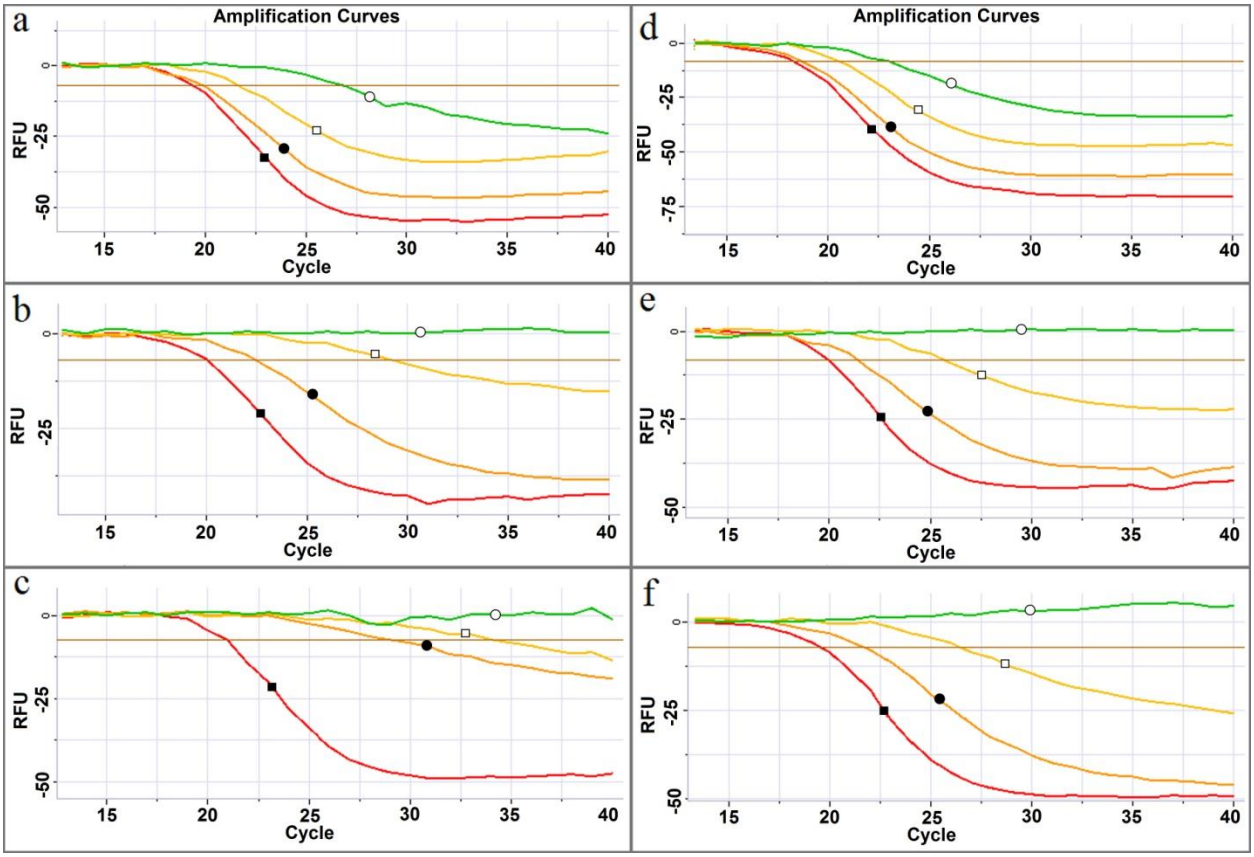

Figure 1: Amplification curves of 53% GC (a-c) and 32% GC (d-f) with collagen at 0 (red ■), 87.5 (orange ●), 100 (yellow □) and 112.5ng/µL (green ○). This figure illustrates how DNA-interacting inhibitor effects can be stronger depending on the amplicon sequence. The 53% GC amplifications performed less well when directly compared to those of 32% GC in amplicons of the same size (a, d 80bp amplicon; b, e 160bp amplicons; c, f 230bp amplicons).

This document is a research report submitted to the U.S. Department of Justice. This report has not been published by the Department. Opinions or points of view expressed are those of the author(s) and do not necessarily reflect the official position or policies of the U.S. Department of Justice.

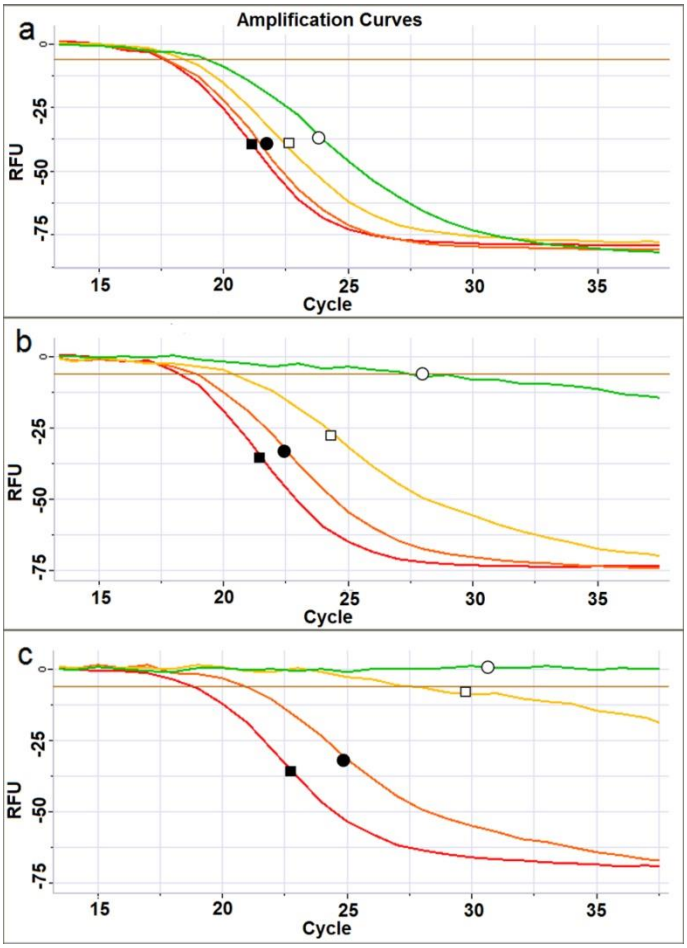

Figure 2: Top panel shows amplification with 80bp (a) , middle panel amplification with 160bp amplicon (b) and bottom using 230bp amplicon (c) 32% GC sequence with bile salts at 0 (red ■), 0.5 (orange ●), 1.0 (yellow □), 1.5ng/µL (green ○). As amplification size increases, the reaction is more prone to failure at lower concentrations of inhibitor.

C_t values

In this study, the changes in C_t between the control and the concentration in which 50% inhibition occurred were more pronounced in the 230bp amplicon for all of the inhibitors typed, but some sequences had greater shifts in the smaller amplicons, as indicated in Table 2. Expectedly, the *Taq* inhibitor, tannic acid, showed minor changes in C_t of 3 to 4 cycles; however, guanidinium and humic acid also showed some smaller C_t shifts, especially at lower concentrations. As guanidinium has been characterized as a mixed mode inhibitor that binds DNA, it was expected to produce greater changes in C_t with increased

This document is a research report submitted to the U.S. Department of Justice. This report has not been published by the Department. Opinions or points of view expressed are those of the author(s) and do not necessarily reflect the official position or policies of the U.S. Department of Justice.

inhibitor concentration, however little change was seen. Presumably this was due to its ability to also act as a protein and a DNA denaturant [16], Thus the DNA was more available at lower guanidinium concentrations, which decreased the C_t value. Then, with the increasing subsequent concentrations, the C_t values began to rise, resulting in no apparent shift in C_t values at the second inhibitor concentration. The DNA interacting inhibitors collagen and bile salts were capable of delaying the C_t by as much 10 to 15 cycles between the control and the second inhibitor concentrations in Table 1, respectively. Bile salts and melanin saw the greatest increase in C_t from the control to the second inhibitor concentration in the 53% GC sequence 230bp IPC amplicon, while the largest effect was seen in collagen with the 160bp 53% GC IPC amplicon.

The other inhibitors produced greater increases in the same interval with the 32%GC 230bp amplicon. In general the changes in C_t were dependent on the type of inhibitor present. For example, in melanin the largest amplicons produce the greatest change in C_t with increased inhibitor concentration regardless of sequence. However this cannot be said for all inhibitors. Tannic acid, collagen and hematin, produced the greatest changes in C_t for the small and medium sized amplicons (Table 2).

Melt Curves

Melt curves are also capable of indicating the possible presence of PCR inhibitors, because it is possible to detect changes in the melt temperature but not in amplification. This happened notably with the addition of collagen and guanidinium. At the lowest concentrations, these inhibitors produced little change in C_t or efficiency, but large changes of 1-2˚C were seen in T_m when compared to the control (Figures 3 & 4). Although the sample's IPC was to able fully amplify, the presence of these inhibitors may still cause issues in downstream applications such as STR genotyping. Another interesting melt curve pattern came from bile salts (Figure 5). With this inhibitor the melt curves indicated an initial decrease in T_m from the control with the first inhibited concentration from Table 1, but unlike collagen and guanidnium, it did not continue changing in the same direction with subsequent increases in bile salts. The greatest changes in melt temperature were found for the inhibitors guanidinium and collagen with

This document is a research report submitted to the U.S. Department of Justice. This report has not been published by the Department. Opinions or points of view expressed are those of the author(s) and do not necessarily reflect the official position or policies of the U.S. Department of Justice.

shifts of approximately 2°C between the control and second inhibitor concentration. The addition of bile salts produced the greatest shift in melt temperatures with the 160bp amplicon in all three IPCs, with the 53% GC sequence showing the largest shift. Collagen had equally large melt shifts with the 160 and 230bp amplicons for the 32% sequence the 230bp amplicon in the 44% GC sequence.

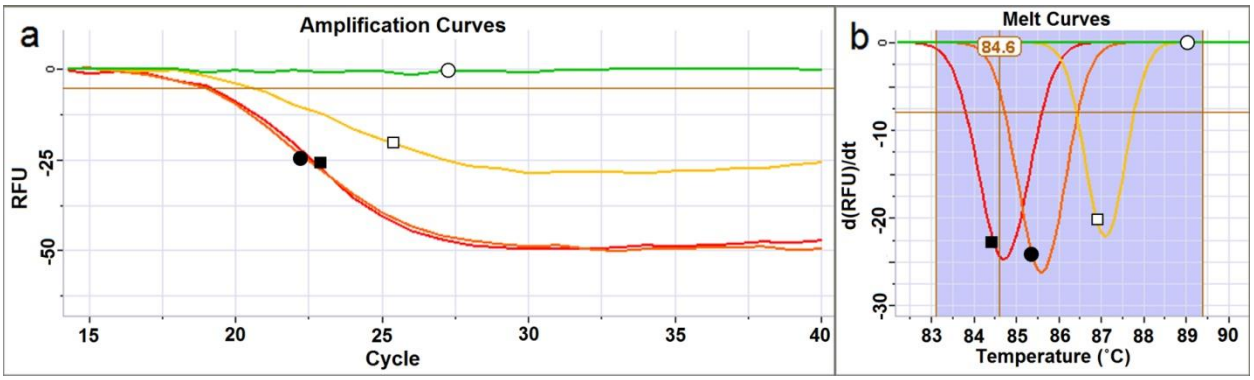

Figure 3: Amplification and melt curves of IPC 53% 160bp amplicon with guanidinium concentrations at 0 (red ■), 1.5 (orange ●), 4.5 (yellow □) and 7.5ng/µL (green ○). This set of amplification curves shows how at low amount of inhibition, it is possible to not detect it during the amplification phase (a), but using melt curves, it is possible to differentiate between an inhibited and uninhibited sample (b).

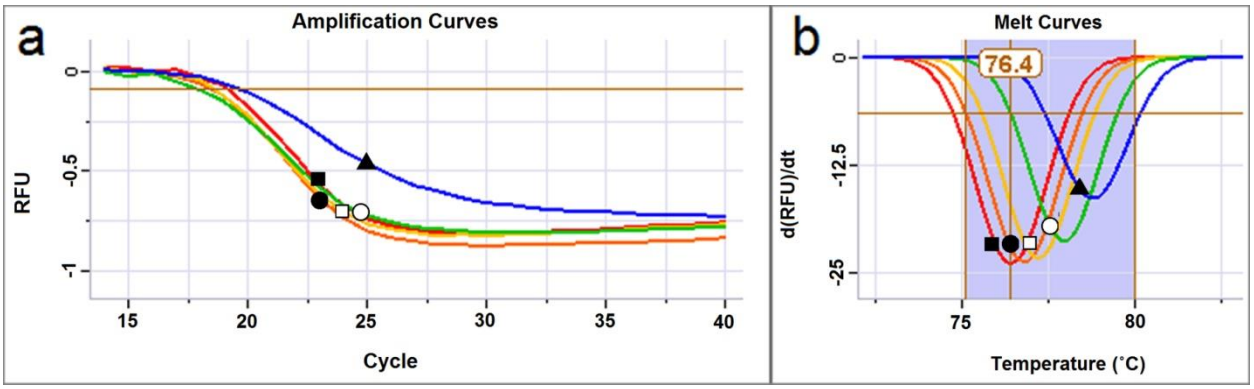

Figure 4: Amplification and melt curves of 44% GC and 80bp amplicon with 0 (red ■), 25 (orange ●), 50 (yellow □), 75 (green ○) and 100ng/µL (blue ▲) of collagen. With the IPCs, increasing concentrations of collagen show little change from the control while the melt curves shift greatly with increasing inhibitor concentration.

This document is a research report submitted to the U.S. Department of Justice. This report has not been published by the Department. Opinions or points of view expressed are those of the author(s) and do not necessarily reflect the official position or policies of the U.S. Department of Justice.

Efficiency values

Changes in reaction efficiency can be traced by modeling each PCR amplifications using the Weibull function $y = a - b^{(-cx^{\wedge}d)}$ [15]. The a and b values correspond to the initial and final fluorescence values, respectively, while the c value follows the changes in C_t. The d value in the model describes the efficiency of the reactions, as it relates to the slope of the curve in the linear phase. In all experiments the value obtained for the control reactions with no inhibitor present were assumed to provide 100% efficiency. The ratios of all subsequent inhibited reactions' d values to their respective control values were used to describe the efficiency of the inhibited reaction as a percentage of the control, as seen in Table 4. The d values generally started from -3 to -4 with the control and rose to 0 as the inhibitor concentration increased and the efficiency of the PCR reaction was reduced. This change was seen more readily as the amplicon lengths increased as well as in amplicons with lesser GC content.

Tannic Acid		53% GC 80bp	53% GC 160bp	53% GC 230bp	44% GC 80bp	44% GC 160bp	44% GC 230bp	32% GC 80bp	32% GC 160bp	32% GC 230bp
d	control	-3.88	-3.73	-3.43	-4.05	-4.09	-3.76	-4.54	-5.33	-4.62
	7.5ng/ul	-3.09	-3.13	-2.63	-3.85	-3.02	-2.68	-3.91	-3.84	-3.34
	11.25ng/ul	-2.47	-2.28	-1.81	-3.06	-2.49	-1.89	-3.06	-2.76	-2.41
	18.25ng/ul	-0.78	-0.58	-0.20	-0.97	-0.75	-0.66	-1.68	-0.26	-0.93

Table 5: An example of the Weibull values obtained for the variable d in the inhibitor tannic acid. As the concentration of the inhibitor increases, the d value increases to 0.

This document is a research report submitted to the U.S. Department of Justice. This report has not been published by the Department. Opinions or points of view expressed are those of the author(s) and do not necessarily reflect the official position or policies of the U.S. Department of Justice.

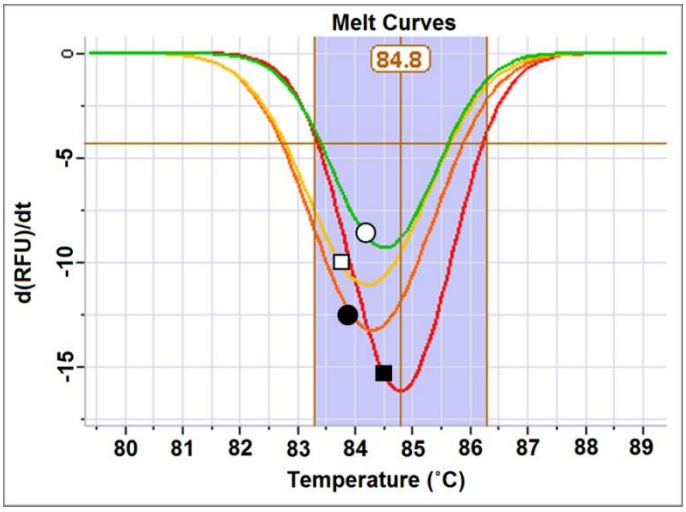

Figure 5: Melt curve effects of bile salts on 53% GC 160bp at concentrations of 0 (red ■), 0.5 (orange ●), 1.0 (yellow □) and 1.5ng/µL (green ○) indicating an initial decrease in T_m followed by a gradual increase in T_m as inhibitor concentration increases. From this, it is possible that the melt may not give any indication to the presence of bile salts if the concentration is sufficiently high.

Conclusion

In our results we show that while the influence of PCR inhibitors on real time amplification is responsive to differences in DNA sequence, size is a much more dominating factor. This is an important issue, as current real time PCR kits vary with respect to the size of their IPC length and sequence, and thus may produce disparate responses to inhibition. Examining amplification efficiency across all of the IPC sequences and amplicon sizes, (Figure 6) we find that as amplicon size increases, and amplicon GC content decreases, inhibitory effects become more detectable.

This document is a research report submitted to the U.S. Department of Justice. This report has not been published by the Department. Opinions or points of view expressed are those of the author(s) and do not necessarily reflect the official position or policies of the U.S. Department of Justice.

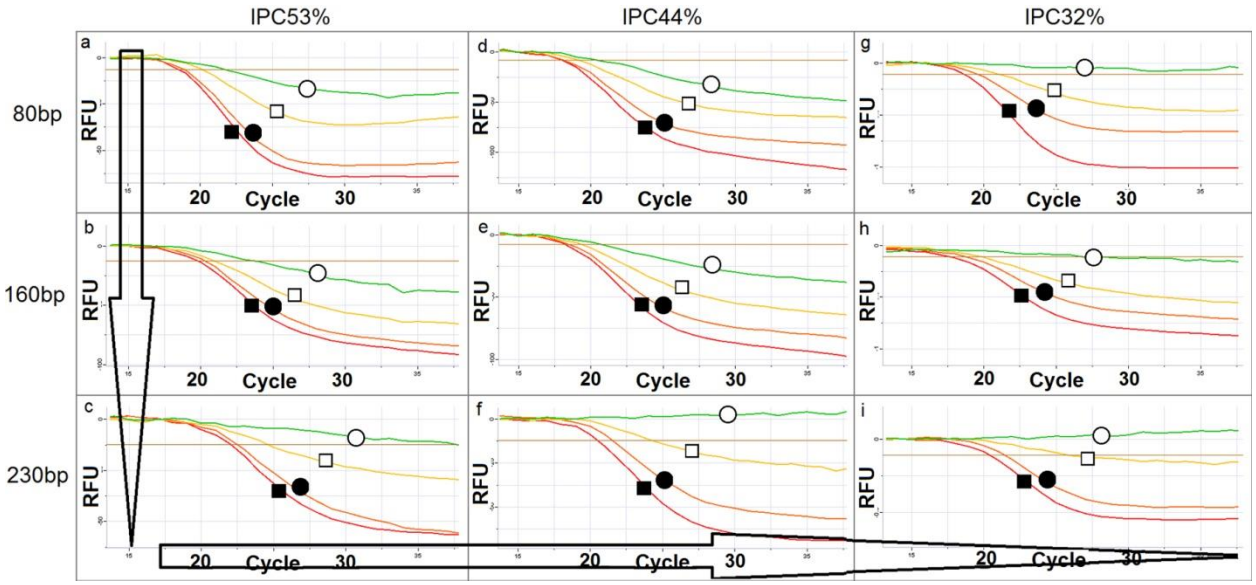

Figure 6: Combined effects of amplicon size and sequence in urea at concentrations of 0 (red ■), 100 (orange ●), 300 (yellow □) and 500mM (green ○) indicating that as the amplicon size increases and as the sequence %GC content decreases, the DNA's sensitivity to inhibition can increase.

Thus the use of a long, low GC content DNA amplicon as an internal PCR control will generally provide an increased ability to detect inhibition during the real time PCR quantification step. Furthermore, our results suggest that it should be possible to tailor the composition of IPCs in quantification kits to a desired level of sensitivity by altering the length of the internal control sequences.

Acknowledgements

The authors would like to thank Giri Narasimhan for creating the random sequence generator program, George Duncan for assisting with computer simulations, Robyn Thompson for the preliminary inhibitor concentrations, the FIU Statistical Consulting Center, and Promega Corporation for their help and technical support in this project. Margie Phipps is acknowledged for technical editing and review. This project was funded through Award No. 2010-DN-BX-K204 of the National Institute of Justice. Points of view in the document are those of the authors and do not necessarily represent the official view of the US Department of Justice.

This document is a research report submitted to the U.S. Department of Justice. This report has not been published by the Department. Opinions or points of view expressed are those of the author(s) and do not necessarily reflect the official position or policies of the U.S. Department of Justice.

References

[1] K.L. Opel, D. Chung, B.R. McCord. A study of PCR inhibition mechanisms using real time PCR, J. Forensic Sci. 55 (1) (2010) 25–33.

[2] P.M. Fulmer, D. Rabbach, K. Huston, G. Saldanha, C. Sprecher. PowerPlex®16 System Validation. Promega Corporation. (2006).

[3] R.L. Green, I.C. Roinestad, C. Boland, L. Hennessy. Developmental Validation of the Quantifiler™ Real-Time PCR Kits for the Quantification of Human Nuclear DNA Samples. J Forensic Sci, 50 (4) (July 2005) 1-17.

[4] M.E. Funes-Huacca, K. Opel, R. Thompson, B.R. McCord. A comparison of the effects of PCR inhibition in quantitative PCR and forensic STR analysis. Electrophoresis 32 (2011) 1084–1089.

[5] R.P. Verkooyen, A. Luijenijk, W.M. Huisman, W.H.F. Goessens, J.A.J.W. Kluytmans, J.H. Van Rijsoort-Vos, et al. Detection of PCR Inhibitors in Cervical Specimens by Using the AMPLICOR Chlamydia trachomatis Assay. Journal of Clinical Microbiology, 34 (12) (Dec 1996) 3072–3074.

[6] J.J. Mulero, C.W. Chang, R.E. Lagac, D.Y. Wang, J.L. Bas, T.P. McMahon, et al. Development and Validation of the AmpFlSTR MiniFilerTM PCR Amplification Kit: A MiniSTR Multiplex for the Analysis of Degraded and⁄or PCR Inhibited DNA. J Forensic Sci, 53 (4) (July 2008) 838-851.

[7] Available at http://blast.ncbi.nlm.nih.gov/Blast.cgi

[8] Available at http://www.idtdna.com/site

[9] Available at http://frodo.wi.mit.edu/primer3/input.htm

[10] Available at https://www.biosearchtech.com

[11] Promega Corporation. Plexor® HY System for the Applied Biosystems 7500 and 7500 FAST Real-Time PCR Systems, Technical manual Part# TM293.

[12] Promega Corporation. Plexor® Analysis Software, Forensic Release version 1.5.4.18. available at http://www.promega.com/resources/tools/plexor-analysis-software-forensic-release/

[13] R. Thompson, G. Duncan, B.R. McCord. An investigation of PCR inhibition using Plexor based quantitative PCR and short tandem repeat amplification. J Forensic Sci. in press.

[14] D.G. Hyams. "CurveExpert Professional" available at http://www.curveexpert.net/

[15] M.W. Pfaffl. Quantification strategies in real-time PCR. Chapter 3 in: S.A. Bustin, editor. A-Z of quantitative PCR. International University Line (IUL) La Jolla, CA, USA. 2004, pp. 87 – 112.

[16] R. Boom, C.J.A. Sol, M.M.M. Salimans, C.L. Jansen, P.M.E. Wertheim-van Dillen, J. van der Noordaa. Rapid and simple method for purification of nucleic acids. J. Clin. Microbiol. 28 (3) (1990) 495–503.

This document is a research report submitted to the U.S. Department of Justice. This report has not been published by the Department. Opinions or points of view expressed are those of the author(s) and do not necessarily reflect the official position or policies of the U.S. Department of Justice.

Part III. Conclusions

Discussion of findings: In general, our results clarify the role of PCR inhibitors in PCR amplification and their effects on STR amplification. We see three basic types of inhibitors – DNA binding, Polymerase binding and mixed mode (inhibitors which affect both polymerase and template) We note that real time PCR amplification efficiency and melt curves help to elucidate the modes of inhibition and have some predictive power in defining downstream allele dropout. Furthermore we note that while allele sequence has an effect on sensitivity to PCR inhibition, the length of the amplicon is most important. Overall we find that PCR inhibition is a complex process that cannot be modeled by one specific compound. Individuals interested in validating new forensic methods should carefully choose a range of inhibitors to encompass the range of modes of inhibition.

Implications for policy and practice: The results of the research clearly show that individuals and companies designing new forensic kits must consider the differential effect of inhibitors when designing new STR kits. A variety of inhibitors should be tested in validation including Taq inhibitors, DNA binding inhibitors and mixed mode inhibitors. The data on size and sequence of control DNA indicates the important effect of amplicon length on PCR inhibition. Designers of real time PCR kits who wish to optimize the length and size of their internal control sequences can utilize this data to develop better quantification kits. Lastly the results comparing the effects of different classes of inhibitors on the recovery of DNA help to instruct the triers of fact on interpretation of difficult partial profiles and indicate that both degradation and inhibition can effect the recovery of larger alleles.

Implications for further research: Future work should continue promising aspects of PCR enhancers and new buffer systems in improving STR amplification. Recent commercial activity validates this approach, with newer kits being far more resistant to inhibition and the widespread adoption of solid phase magnetic bead based methods for DNA extraction.

This document is a research report submitted to the U.S. Department of Justice. This report has not been published by the Department. Opinions or points of view expressed are those of the author(s) and do not necessarily reflect the official position or policies of the U.S. Department of Justice.

Part IV: Dissemination of Research Findings

Publications

Pionzio, A. ; McCord, B. The Effect of Internal Control Sequence and Length on the Response to PCR Inhibition in Real-Time PCR Quantitation, *FSI: Genetics* Volume 9, March 2014, Pages 55–60.

Thompson, R. Duncan, G. McCord, B. An investigation of PCR inhibition using Plexor® based quantitative PCR and short tandem repeat amplification, *J. Forensic Sci. in press.*

Wang, J; McCord, B; The application of magnetic bead hybridization for the recovery and STR amplification of degraded and inhibited forensic DNA, *Electrophoresis*, **2011** *32(13)*, 1631–1638.

McCord, B. R.; Buel, E. Analytical Techniques/Capillary Electrophoresis in Forensic Biology, In *Encyclopedia of Forensic Sciences*; (2nd edition) Jay Siegel and Pekka Saukko, ed., Academic Press, San Diego, CA, 2013,394-401.

Robyn Thompson; Silvia Zoppis; Bruce McCord, An Overview of DNA Typing Methods for Human Identification: Past, Present, and Future *DNA electrophoresis protocols for Forensic Genetics*. Alonso, A., ed. Methods in molecular biology, Springer protocols, Human Press, New York, 2012 3-16.

Presentations

Bruce McCord, Analysis of Degraded DNA, Oklahoma State University May 7, 2010

Bruce McCord, The application of RT-PCR meld curves in the determination of PCR inhibition, Forensica 2010 Telc, Czech Republic May 24-26, 2010

Bruce McCord, The development of methods for genotyping degraded DNA, International Forensic Science Symposium, University of Amsterdam, Amsterdam, Netherlands May 27, 2010

Bruce McCord, Robyn Thompson, Kerry Opel, Maribel Funes, and Silvia Zoppis, The application of RT-PCR meld curves in the determination of PCR inhibition, 2010 NIJ Conference, Washington, DC June 14-16, 2010

Bruce McCord, Robyn Thompson, and Kerry Opel, An examination of PCR Inhibition in forensic DNA genotyping by rt-PCR and CE, CE-ITP Baltimore, MD August 30-Sept 1, 2010.

Robyn Thompson and Bruce McCord, An Analysis of Binding Mechanisms for Real-Time Polymerase Chain Reaction(PCR) Inhibition Using Efficiency and Melting Curve Effects, Promega San Antonio TX October 11-13, 2010

Thompson, R.; McCord, B. An Analysis of Binding Mechanisms for Real-time Polymerase Chain Reaction (PCR) Inhibition using Efficiency and Melting Curve Effects, AAFS, Chicago, IL February 22, 2011

Bruce McCord, A workshop on capillary electrophoresis in forensic analysis, FBI Laboratory, Quantico, VA, August 29-30, 2011.

This document is a research report submitted to the U.S. Department of Justice. This report has not been published by the Department. Opinions or points of view expressed are those of the author(s) and do not necessarily reflect the official position or policies of the U.S. Department of Justice.

Bruce McCord , Developing an understanding of PCR inhibition using real time PCR and melt curve analysis, International Symposium on Human Identification, Washington, DC, October 3-6, 2011

Bruce McCord and John Butler, Post symposium workshop, Troubleshooting Laboratory Problems, International Symposium on Human Identification, Washington, DC, October 3-6, 2011

Bruce McCord, Capillary electrophoresis for DNA analysis, Presymposium workshop, Latin American Conference on Capillary Electrophoresis, Hollywood beach, FL Dec 2-6, 2011

Bruce McCord, Developing an understanding of PCR inhibition using real time PCR and melt curve analysis, Latin American Conference on Capillary Electrophoresis LACE Dec 2-6, 2011

Bruce McCord, DNA typing of degraded and inhibited samples, Chinese Academy of Sciences, Beijing China July 15, 2012

The effects of DNA sequence and length on inhibitor interactions in real time PCR amplification, Arianna Pionzio and Bruce McCord, International Symposium on Human Identification, Nashville, TN Oct 7-10, 2012

Bruce McCord, "Using Curve Fitting Models to Assess PCR Inhibition in Forensic Samples, the NIJ Conference, Arlington, VA, June 18-20, 2012

Bruce McCord, Troubleshooting STR systems, Promega Latin American workshop on Human Identification, Miami, Florida August 31, 2012

Bruce McCord, PCR inhibition, Qiagen Users Forum, Hilden, Germany, March 13-14 2012

Bruce McCord, Promega Workshop on DNA typing, Mexico City, Mexico June 2013

Bruce McCord, Workshop on capillary electrophoresis and setting instrument thresholds, Miami Dade Police Laboratory, July, 23, 2013

Bruce McCord, Troubleshooting DNA Typing Systems, Bode Mid-Atlantic Symposium, Charlottesville, VA, Sept 23-25, 2013

Bruce McCord, Workshop on Mixture Identification, International Symposium on Human Identification, Atlanta, GA, October 7-10, 2013

Bruce McCord, An introduction to DNA typing and its application in the analysis of degraded and inhibited samples, U Southern Mississippi, Hattiesburg, MS, November 8, 2013.

Bruce McCord, Setting Thresholds, Workshop on DNA typing methods, NC State Crime Laboratory, Raleigh, NC, Dec 9-10, 2013.

Bruce McCord, Forensic DNA analysis and its application to degraded and inhibited DNA, University of Nebraska , Lincoln, NE, April 17-18, 2014

This document is a research report submitted to the U.S. Department of Justice. This report has not been published by the Department. Opinions or points of view expressed are those of the author(s) and do not necessarily reflect the official position or policies of the U.S. Department of Justice.